CHITOSAN SUPRAMOLECULAR ORDERING AS A FUNCTION OF ITS MOLECULAR WEIGHT

Emmanuel BELAMIE [1,3], Alain DOMARD[1], Henri CHANZY[2] and Marie-Madeleine GIRAUD-GUILLE[3]

(1) Laboratoire d'Etudes des Matériaux Plastiques et des Biomatériaux (UMR CNRS 5627), Université C. Bernard, 43 Bd du 11 Novembre 1918, 69622 Villeurbanne Cedex, France.(2) CERMAV (CNRS) Université J. Fourier- BP 53 - 38041 Grenoble Cedex 9, France.(3) EPHE, Université P.&M. Curie (URA CNRS 2156), 66650 Banyuls-Sur-Mer, France.

Abstract

The supramolecular ordering of chitin in arthropods cuticle is that of a stabilized analogue of cholesteric liquid crystals. In-vitro studies have been conducted on chitin crystallites suspensions that demonstrated their ability to self-rearrange with the same molecular ordering as in the original biological tissue. The aim of the present work is to investigate the crystallization behaviour of chitosan from acidic solutions. Liquid and solid crystallizations of polymers were shown in the literature to be often dependant on the molecular weight. We have thus first prepared chitosans with different average DP's by means of an original technique, which is carried out in solid state conditions.

The so-produced oligomers were shown to crystallize in a typical spherulitic manner. The morphology and crystalline structure of the germs were studied either by imaging and diffraction techniques. Polarizing microscopy and metal shadowing of extended molecules allowed us to observe the emergence of germs from isotropic solutions of oligomers and to describe different steps of the spherulite growth at a molecular scale. The relative orientation of the chains within the crystal, as well as the crystalline structure, were elucidated by means of X-Ray and electron diffractions.

Chitosan with a higher molecular weight ($\overline{M_w}$ =1.8 x10^5 g.mol^{-1}) exhibited a rather different behaviour in concentrated solutions. Films prepared by slow evaporation of the solvent were observed in polarizing microscopy before ultra-thin sectioning and observation in TEM. These observations revealed differences in the crystallization pathway of chitosan polymers, mainly depending on the counter-ion initially used for its solubilization.

Introduction

Previous studies on the crystalline structure of chitosan have highlighted the extraction and precipitation conditions leading to different polymorph chitosan crystals. Some of them were carried out on the material derived from chitin by heterogeneous extraction processes. It was thus supposed to have kept the original structure of chitin in the cuticule of arthropods. The so-called tendon polymorph was identified by Ogawa *et al.* in 1984. Other polymorphs were described that were obtained either by

heating the chitosan, leading to the so-called annealed polymorph, or by dissolution and then film-casting or re-crystallization. Samuels reported (1981) the influence of the preparation process on the structure of the observed films from the molecular to the macroscopic levels and described different polymorphic crystal forms as well as morphological structures varying from spherulites to rods. Lamellar crystals with the typical tendon polymorph crystalline structure were obtained by Cartier *et al.* (1990) by precipitating solutions of short oligomers in hot concentrated ammonia and under pressure. The aim of the present work is to investigate the molecular organization of low molecular weight chitosan that was re-crystallized at room temperature and pressure. Optical and electron microscopic observations were performed to describe the samples on a morphological point-of-view. The crystalline structure and a possible interaction with water were determined by means of X-Ray and selected area electron diffraction.

Results and discussion

Morphological aspects

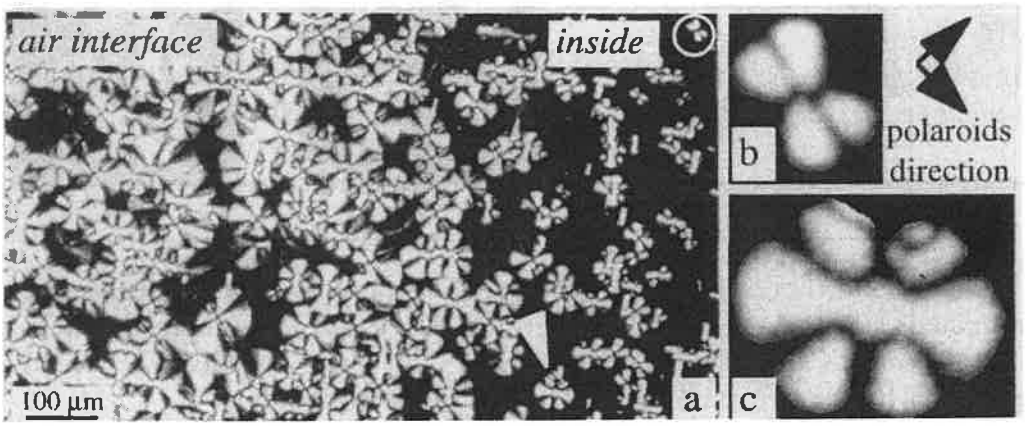

Figure 1 a-c. Oligomers solution at 1% by weight observed between slide and coverslip in polarized light. Figure 1b and 1c are views at higher magnification of the germs marked on figure 1a with the white circle and the white arrow head respectively

When placed between partially sealed slide and coverslip, solutions are allowed to dry, with a more or less progressive evaporation of the solvent. Figure 1 shows a pattern typically observed, in optical microscopy between crossed polaroids, with solutions of chitosan oligomers at concentrations ranging from 1% to 4% in weight. The edge of the coverslip, *i.e.* the air interface, is on the left of the photograph, the inside of the preparation is on the right. In optical microscopy between crossed polars, isotropic domains lack birefringence and remain dark, whereas anisotropic domains appear bright, except for certain positions depending on the

orientation of the index ellipsoid. The first is when the largest axis of the ellispoid is lying parallel to the optical axis, *i.e.* perpendicular to the preparation plane. The two others are direct consequence of the polarizing technique, since these extinctions occur when the major axis is oriented in the same direction as one of the polaroids. At low magnification the photograph of figure 1a shows large domains, mainly inside the preparation, that remain dark and correspond to amorphous zones, as confirmed by rotating the microscope stage around the optical axis.

Birefringent domains nucleate and grow between slide and coverslip near the air interface. On the right of the photograph, they have the form of small rod-like or fan-shaped germs, depending on their growth stage and their orientation with respect to the polaroids. Near the air interface the germs are disk-like and often fuse to form a mosaic of bright domains separated by sinuous extinction lines. We present on figures 1b and 1c two typical germs viewed at a higher magnification.

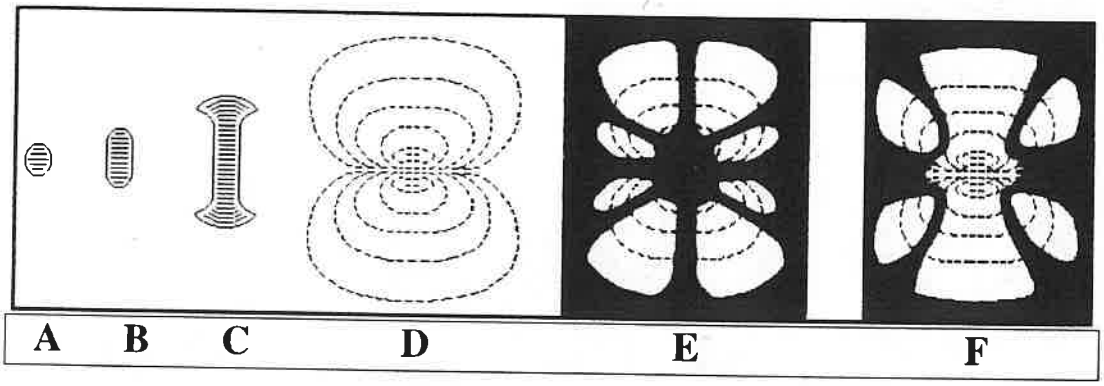

Figure 2. Schematic representation of the growing process of a spherulitic germ from the nucleus stage (A) to the final spherulite (D). E and F are representations of the theorical patterns that should be observed with such crystals when seen in polarized light with the two extreme orientations of the polaroids.

These patterns are typical of a spherulitic crystallization. The different germs we observe on figure 1 correspond to different steps of the crystal growth. We propose that chitosan oligomers follow the model of spherulite growth proposed by Keller (1955) and presented on Figure 2. During evaporation of the solvent, germs can arise from the solution and, depending on different conditions that we shall discuss further, they can more or less developp and form either individual rods or a mosaic of connected spherulites.

In some cases, it is possible that, the oligomers concentration being large enough, spherulites can superimpose. The subsequent addition or substraction of optical path difference in the width of the preparation could thus explain the complexity of the patterns seen on the left on figure 1a.

Although it is now established that chitosan oligomers crystallize in the form of spherulites, we had to determine the molecular orientation of polymer chains within the supramolecular structure. The introduction of a

first order retardation plate (λ) led us to conclude that the spherulites have their larger refractive index in the tangential direction and thus have a negative birefringence. This is consistent with the growing sequence presented on figure 2 and with the molecular orientation we propose for the final spherulite (2D).

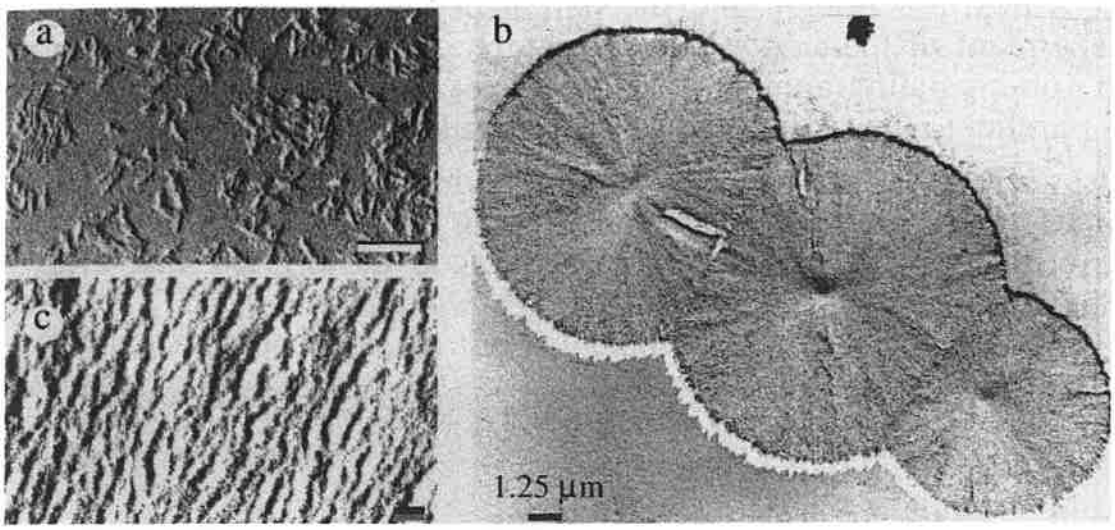

Figures 3 a-c. Micrographs obtained in TEM after metal shadowing. (a): individual rod-like germs, bar = 0,2µm. (b): three well-formed spherulites. (c) same as (b) at a higher magnification, bar = 50 nm.

Samples were then observed in TEM after shadowing with platinum. Figure 3a diplays a situation where only small individual rod-like germs are visible. They are almost 20 nm in width with no particular orientation in the field of view. Different intermediate steps where observed that are not presented here but are in good agreement with the model of growth presented above.

The well formed spherulites of figure 3b exhibit a parallel striation, whose periodicity is about the width of an individual rod-like germ, and is close to 20 nm. The striation is parallel to the long axis in the center and spread out to the edges, keeping almost perpendicular to the border.

When looking carefully to the ridges, one should observe that their orientation is not always exactly parallel to the radius but often make a small angle around this direction. This is particulary visible on the photograph of figure 3c.

In addition, the shadow obtained after metal evaporation gives a width of the spherulite between 20 and 30 nm. When this value is compared to the average radius (10 to 15µm), it clearely appears that the structure is essentially flat, and thus that the crystallization was mainly two-dimensionnal.

The small individual germs are probably formed by a lateral aggregation of oligomer chains leading to a rod-like morphology, growing perpendicular to the chain direction in a typical polymer single crystal fashion. The single nucleus then grows in the form of fibrils that repeatedly branch during their growth, so as to fill up the space available. In many other crystalline forms, the nucleus gives rise to a single crystal with all the molecules having the same three-dimensonal orientation. In the case of spherulites, the branch and the parent crystallite make a certain angle, independant of their crystalline structure. Although the branching is thus said non-crystallographic, the major axis of the crystallites remains more or less parallel to the radii of the whole spherulite.

Crystallographic aspects

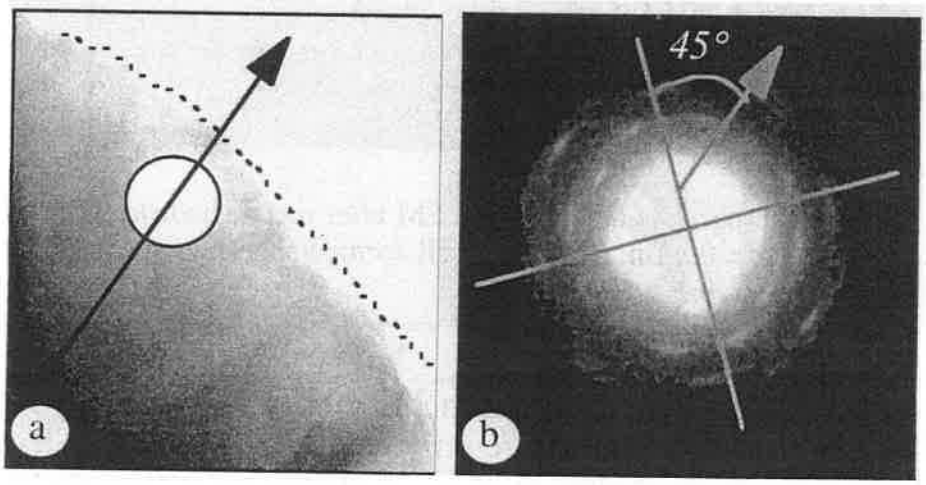

Figure 4a. Electron micrograph taken near the edge of a spherulite and recorded without shadowing. The white circle represents the electron beam trace and the black arrow gives the direction of the radius of the germ.
Figure 4b. Electron diffraction pattern taken in the region of the spherulite presented on figure 4a, and plotted with the correct orientation against the micrograph.

Electron diffraction was performed on selected areas, in order to investigate the crystalline structure and the molecular orientations of the spherulites at the level of the individual rods that lead to the striated pattern. Samples were submitted to low-dose irradiation and couples of photographs were recorded in both imaging and diffraction modes, allowing us to specify the molecular orientation in each region of the spherulite.
The samples observed directly after preparation of the spherulite and kept dry under vacuum gave broadly defined diffraction patterns (not shown), with essentially 4 reflexion dots whereas samples hydrated overnight gave

much more defined patterns with about 30 reflexions dots equivalent four by four. These results, together with X-Ray diffraction experiments (not presented) give an evidence for the presence of water in the normal crystal lattice. When placed under vacuum, water is removed and the intensity of the diffracted beam decreases.

When the diffraction diagrams, recorded on selected areas, are printed with the correct orientation with respect to the images, it comes out that the two major orientations defined by the four bright diffraction dots are lying at an angle of about 45° with respect to the direction of the long axis of the spindle-like individual units. An example is given with figure 4b, which is printed beside figure 4a the region were it was taken. This lets us suppose that in each individual unit, molecules are lying perpendicular to its long axis and parallel to c axis, thus perpendicular to the plane of observation. That the diffraction diagrams are constituted by dots and not spots is probably because, in the selected areas, the crystallites are not exactly aligned in the same direction, which is consistent with what we observed in imaging electron microscopy on figure 3c. When we calculate the length of the dots and interprete it in terms of angular variation of the crystallite orientation, we found a value near 30°, meaning an angular variation of 15° around the average direction. It is noteworthy that this result is in very good agreement with the angular spreading of the elemental units measured on figure 3c, which is also near 15° from the average orientation. This is also consistent with the typical growing process of spherulites which implies the non-crystallographic branching of new crystallites on parent ones, as explained in the previous section.

Conclusions

It was demonstrated in this study that chitosan oligomers are able to crystallize in the form of spherulites. These crystalline structures were described either in optical microscopy in polarized light and by electron microscopy after metal shadowing. The observations made with both techniques gave consistent data about their morphology. The latter technique was shown to be an accurate one that allows us to describe more precisely, at the molecular level, the birefringent objects revealed and studied by means of the former.

Such a spherulitic behavior is widely observed in the field of natural and synthetic polymers. We can mention for instance cellulose for natural polymers, and polyethylene for synthetic ones. In both cases, as in many others, a great number of studies have been carried out that led to the quite complete understanding of either the crystallization process and the molecular organization. It seems that chitosan oligomers behave almost like several other polymers.

Nevertheless, it is known that for most polymers, the direction of the highest refractive index coincides with the chain direction because most of the covalent bonds are aligned with this direction. We have shown by electron diffraction that the molecules are lying perpendicular to the observation plane, and the birefringence observed in polarizing microscopy is thus not due to the refractive index along the chain. It is more likely that, because of some hydrogen bonding within the crystalline structure and/or the presence of the NH_3^+ polarized group, the refractive index is large enough in one of the directions perpendicular to the chain axis compared to those in the other lateral directions. The material is therefore said to be biaxal, meaning that the index ellipsoid do not exhibit any rotational symmetry about any of its three principal axis. The orientation determined by means of the first order retardation plate should thus not be directly related to the long axis of the chains but to molecular interactions in a perpendicular direction.

In addition, we have shown, either by X-Ray diffraction and electron diffraction, that a water molecule is probably inserted in the crystal lattice. This is different from results obtained for example by Cartier *et al.* (1990), and in general high-temperature polymorphs (Mazeau *et al.*, 1994; Yui *et al.* 1994, 1995), who do not observe any difference between diffraction patterns obtained either with hydrated or anhydrous crystals.

Acknowledgment

We thank Y. Bouligand for fruitful discussions about molecular ordering and his help in polarized light microscopy interpretation.

References

(1) **Cartier**, N., Domard, A. and Chanzy, H. (1990), *Int. J. Biol. Macromol.*, **12**, 289-94.
(2) **Keller**, A. (1955), *J. Polym. Sci.*, **17**, 291.
(3) **Mazeau**, K., Winter, W.T. and Chanzy, H. (1994), *Macromolecules*, **27**, 7606-12.
(4) **Ogawa**, K., Hirano, S., Yui, T. and Watanabe, T. (1984), *Macromolecules*, **17**, 973-15.
(5) **Samuels**, R. J. (1981), J. Polym. Sci., Polym. Phys. Ed., **19**, 1081-1105.
(6) **Yui**, T., Imada, K., Okuyama, K., Obata, Y., Suzuki, K., and Ogawa, K. (1994), *Macromolecules*, **27**, 7601-7605
(7) **Yui**, T., Ogasawara, T., and Ogawa, K. (1995), *Macromolecules*, **28**, 7957-7958

PERMEABILITY OF CHITOSAN MEMBRANE

Piyabutr Wanichpongpan (1), Suwalee Chandrkrachang (2)

(1) Department of Chemical Engineering, Faculty of Engineering, King Mongkut's Institute of Technology Thonburi (KMITT) Bangkok 10140 Thailand
(2) Bioprocess Technology Program, School of Environment, Resources and Development, Asian Institute of Technology (AIT) Pathumthani 12120 Thailand

Abstract

The chitosan was prepared from local black tiger shrimp shells (*Penaeus monodon*) with the degree of deacetylation of 75.9 %. The concentration of casting solution was 1 % chitosan in 0.5 % acetic acid. The average thickness of the produced membranes was between 30-40 micrometer. The chitosan membranes were also characterized of their mechanical properties and performances. The different concentrations of ammonium sulfate solutions ranging from 1%, 10%, 30% and 50% were set for dialysis through the membranes. During dialysis the constant volumes of water were changed in every interval time of 3, 6, 9, 24 and 30 hours. The result showed the amounts of ammonium sulfate dialysing through the membranes were 54-60%, 28-31%, 4-10%, 1-9% and 0.3-3% in different interval time of 3, 6, 9, 24 and 30 hours respectively. The efficiency of dialysing membrane of ammonium sulfate was highest upto 99.9%. The permeability of the membrane was calculated with the results in the range between 0.22-1.67 liter per square meter per hour (L/m^2 h) during the time of dialysis.

Keyword: Chitin, chitosan, membrane, stress, strain, modulus of elasticity, dialysis, permeability.

Introduction

Chitin is a value-added biopolymer extracted commercially from shellfish wastes. Chitosan is produced from chitin by deacetylation. The commercially useful properties of chitin and chitosan have already been incorporated into products for diverse applications [9]. Chitosan membrane has been studied in various areas [15]. In membrane separation, it has been proposed to use as dialysis memebranes. Dialysis separates solute mixtures on the basis of molecular size and possible molecular conformation and net charge. In dialysis, driving force is the concentration difference that can be used primarily to remove or exchange low-molecular weight solutes from a solution and recovery of bioproducts.

Materials and methods

Preparation and analysis of chitin and chitosan

Chitin was prepared from local black tiger shrimp shells (*Penaeus monodon*) by deproteination in 1 molar sodium hydroxide solution and followed by demineralization

in 1 molar hydrochloric acid. After throughly washed by water until without chloride ions were detected, then the crude chitin was obtained. The process of deacetylation of the chitin was done under 50% sodium hydroxide at ambient condition for 72 hours. The chitosan was obtained after throughly washing out alkaline residue. The drying chitosan was determined some important properties of moisture content, ash content and degree of deacetylation by titration method[15].

Preparation of chitosan membranes

The casting solution was prepared within the concentration of 1% chitosan solution in 0.5% acetic acid by stirring the dissolved chitosan for 24 hours and then filtered for remove out the undissolved particles. The viscosity of the casting solution was measured by Brookfield viscometer model DV-II^{+} within various speed (rpm) and torque (%). The initial viscosity of the casting solution was high value and gradually dropped down along with the storage time. The viscosity of casting solution during preparation the membranes was almost in the metastable state. The membrane casting chamber was set at the conditions of 30-40°C and 55±5 % relative humidity for 48 hours. The drying membranes were neutralized in 10% sodium hydroxide solution and followed by throughly washing in water and drying under pressing hot plate. The smooth surface membranes were obtained within the average thickness of 30-40 micrometer[12,15,16].

Characterization of chitosan membranes

The produced chitosan membranes were kept storage in drying condition for characterization of some physical properties. The water absorption of the membranes was determined by soaking in deionized water overnight. The different in weights and sizes of the membranes before and after water absorption were measured to obtain the water absorption and shrinkage values. The membranes were cut into the size of 0.5 x10 cm in both dry and wet conditions and were measured of the tensile strength by Instron Universal Tester Instrument Model 5583 [2,4,5,12,13,17,18,19,21]. The mechanical properties of applied load, stress, strain and modulus of elasticity were measured and computerized as shown in the result.

Experiment of dialysis ammonium sulfate solutions through chitosan membranes [1,3,10,11,15,20].

The different concentrations of 1%, 10%, 30% and 50% of aqueous ammonium sulfate solution were prepared for determination of the dialysis. The chitosan membranes were fixed to the plastic containers to make a system consisting of two compartments. Each 10 ml of different concentrations of ammonium sulfate solutions were set for dialysis through the chitosan membranes into water compartments. Every interval time of 3, 6, 9, 24 and 30 hours during dialysis, 100 ml of deionized water were changed for analysis of the amount of ammonium sulfate diffusion. The analytical procedure was done by turbidity method adapted from ASTM 1985 [3] and Analytical chemistry of elements [20]. The experimental set-up was shown in Figure 1.

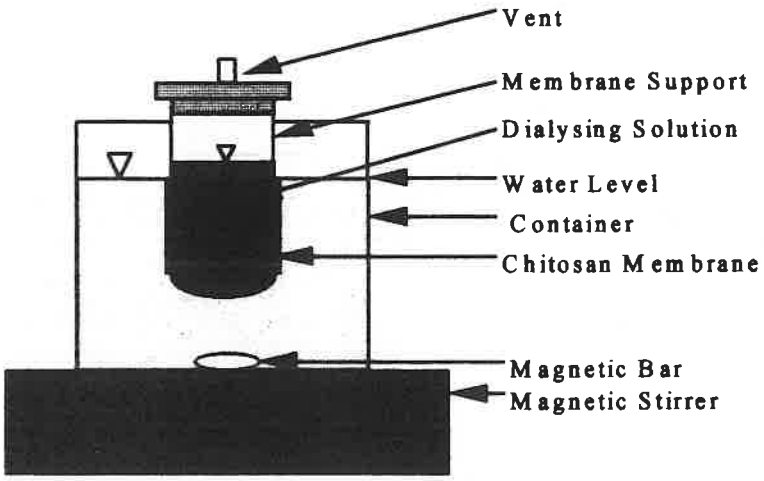

Figure 1 Schematic diagram of the experimental set-up

Results and Discussion

The chitosan was obtained from the process of deacetylation of chitin with the analysis result as shown in Table 1.

Table 1 Characteristics of the prepared chitosan

Chitosan	
Source	Shrimp Shells (*Penaeus monodon*)
Form	Flakes
Colour	White
Yield from Chitin (%)	85
Moisture Content (%)	8.08
Ash Content (%)	0.54
Degree of Deacetylation (%) : Titration Method	75.92
Casting Solution	1% in 0.5% Acetic Acid
Initial Viscosity : Brookfield Model DV-II$^+$ (cps)	673

The chitin is natural biopolymer which extracted from local shrimp shells. The deacetylation of chitin to obtain chitosan might cause the deviation from their nature [16]. The quality of chitin and chitosan is varied seasonally in chemical composition and structure depends on the sources and freshness of raw materials. However, the preparation of chitin and chitosan in this experiment was carefully control of time, concentrations and other conditions for consistantcy of the products in terms of high molecular weight with lowest ash and contaminants.

The result of viscosity measurement of chitosan casting solution was studied for the relationships of shear stress and shear rate of the fluid properties as shown in Table 2 and Figure 2.

Table 2 Viscosity and related fluid properties of chitosan casting solution

Test Number	1	2	3	4	5
Speed (rpm)	10	30	50	60	100
Torque (%)	50.0	67.1	73.2	83.9	94.1
Shear Stress (dynes/cm^2)	23.9	32.0	35.0	40.1	45.0
Shear Rate (s^{-1})	1.1	3.1	5.2	6.3	10.5
Viscosity (cps)	2273	1019	668	639	430

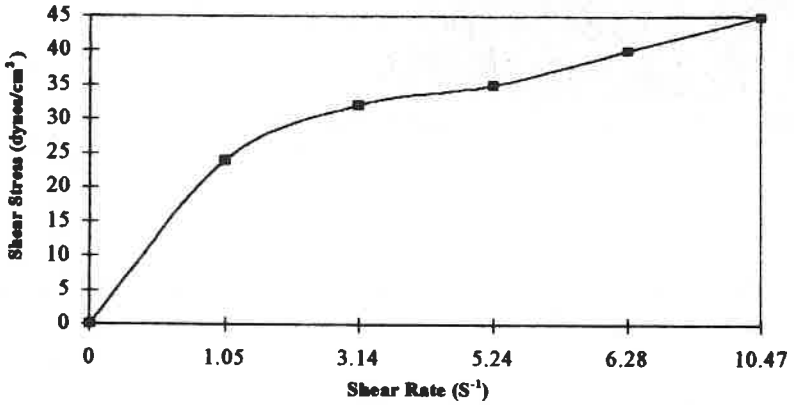

Figure 2 Shear stress and shear rate relationships in chitosan casting solution

The properties of chitosan solution is significantly basic knowledge which is able to express in terms of viscosity measurement for calculation of shear stress and shear rate values. It was found that the relationship between shear stress and shear rate was non-linear relative which referred to non-newtonian fluid character[6,12,14].

The casting membrane method was done by the combination of evaporation and diffusion process which referred to the type of phase-inversion membranes[12]. The membranes exist after gelation and contraction followed by complete drying which are classified as primary gel structures. The effects upon the primary gel structures were illustrated in the increasing degree of swelling capacity, increasing thickness and increasing permeability as shown in the properties of chitosan membrane in Table 3.

Table 3 Water absorption and swelling capacity of chitosan membranes

Weight (g)		Thickness (μm)		Expansion (%)		Water Absorption (%)
Dry	Wet	Dry	Wet	Volume	Area	
0.0233	0.0569	35	55	43.05	10.51	59.03

The tensile strength of chitosan membranes in both wet and dry conditions are shown in Table 4.

Table 4 Mechanical properties of chitosan membranes

Parameters	Dry	Wet
Thickness (μm)	35.00	55.00
Load-mean (N)	14.52	2.86
Stress-mean (MPa)	82.98	10.39
Strain-mean (%)	33.22	119.75
Modulus-mean (MPa)	3620.07	27.85

In drying condition, the chitosan membranes had shown high values of load, stress, strain and modulus. However, for wetting condition, the reduction of the values of load, stress and modulus were shown significantly comparing with the dried membranes. But the strain value of the wet membrane was highest upto 119.75 %. The high strain value of the biomembranes leads to the properties of elasticity for biopolymer. When a uniaxial tensile force is applied to a film, it causes the film to be elongated in the direction of the force and deformation of the film occurs. If the film returns to its original dimensions when the force is removed, the film is said to have undergone elastic deformation. If the film is deformed to such an extent that it cannot fully recover its original dimensions, it said to have undergone plastic deformation. During plastic deformation, the film atoms are permanently displaced from their original positions and take up new positions. The ability of chitosan film to be extensively elastically deformed without fracture is one of the most useful physical properties of membranes[4,5,12,13,17,18,19,21].

The percentages of dialysis of ammonium sulfate solutions through chitosan membranes at different concentrations and times were shown in Table 5.

Table 5 Dialysis of chitosan membrane at different concentrations and time

$(NH_4)_2SO_4$ (%)	% Dialyzing					Efficiency of Dialyzing Membrane (%)
	3h	6h	9h	24h	30h	
1%	58.30	31.20	10.45	7.78	2.95	99.49
10%	54.00	28.30	3.94	9.26	0.32	99.96
30%	60.00	28.30	8.37	2.28	0.52	99.98
50%	57.20	28.10	6.43	1.32	0.35	99.99

The dialysis of ammonium sulfate through the chitosan membrane illustrated the phenomenon of diffusion between the two compartments of salt solutions and deionized water. It was found that the rapid flow of the salt solutions through the membranes was between 54-60% at the first 3 hours and almost reached to the constant diffusion in 24 hours as shown in Figure 3.

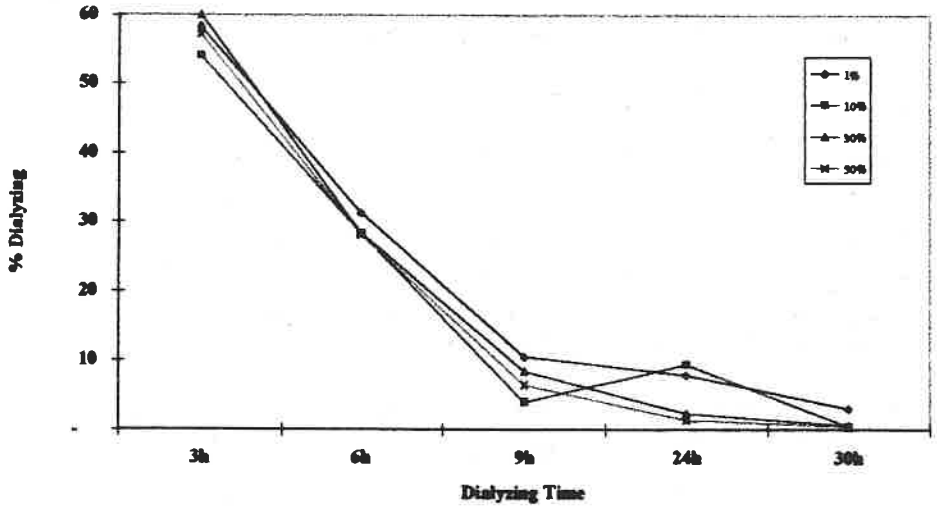

Figure 3 Relationships of percentage of dialyzing at different concentrations and time

The efficiency of the dialysis of chitosan membrane is also shown in Figure 4.

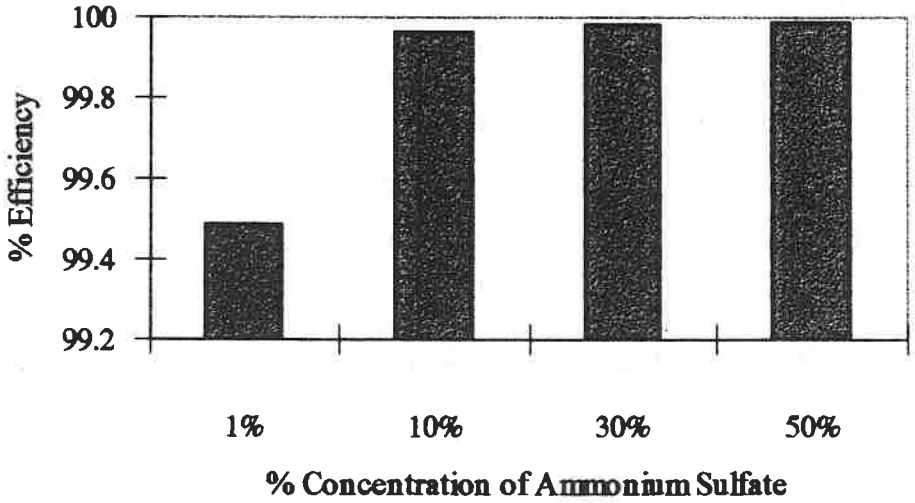

Figure 4 Efficiency of dialysis of chitosan membrane

The permeability of chitosan membrane was calculated by the following equation:-

$$P = \frac{D}{d} = \frac{2.303 V_A V_B}{At(V_A + V_B)} \log \frac{(C_A - C_B)_O}{(C_A - C_B)_t}$$

The two compartments; A and B having volumes and concentrations of V_A; C_A and V_B; C_B ,respectively. The two compartments are separate by chitosan membrane having a thickness; d and cross-section area; A. If the dialysis coefficients; D are equal in each direction and independent of concentration and if the two volumes are constant during dialysis, whereas the subscripts of o and t refer to initial and final condition. The permeability is then proportion of D and d [12]. Thus the measurement of the concentration differences at the start and the end of dialysis can be used to calculate the permeability of the chitosan membranes as shown in Table 6.

Table 6 Permeability of the chitosan membrane at different concentrations and time

$(NH_4)_2SO_4$ (%)	Permeability ($L/m^2 h$)				
	3h	6h	9h	24h	30h
1%	1.58	0.98	0.69	0.25	0.84
10%	1.39	0.88	0.60	0.22	1.15
30%	1.67	0.99	0.69	0.26	1.25
50%	1.53	0.94	0.64	0.24	1.50

The permeability values at each interval time were shown in the curves of relationships of permeability and dialysing time in Figure 5.

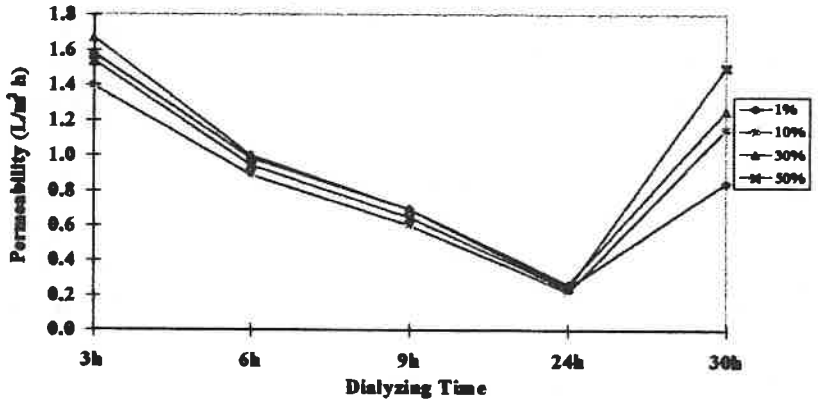

Figure 5 Relationships of permeability at different concentrations and time

The result showed the amounts of ammonium sulfate dialysing through the membranes were 54-60%, 28-31%, 4-10%, 1-9% and 0.3-3% in different interval time of 3, 6, 9, 24 and 30 hours respectively. The efficiency of dialysing membrane of ammonium sulfate was highest upto 99.9%. The permeability of the membrane was calculated with the results in the range between 0.22-1.67 liter per square meter per hour ($L/m^2 h$) during the time of dialysis.

Conclusion

The chitosan membranes which produced from local shrimp shells had shown the property of permeability which allowed the ammonium sulfate salt to pass through. The chitosan membranes also expressed the character of high tensile strength in drying condition as well as high strain value in wetting condition which reflected the property of elasticity. The rate of dialysable ammonium sulfate salt was directly proportional to the concentration difference between the two compartments. The rapid flow of the salt solutions through the membranes was occurred at the initial stage of dialysing time and continued until it reached equilibrium which occurred within the rate of constant diffusion. This advantage on dialysis behavior leads the chitosan membranes are able to apply for separation of some specific proteins from the salt solutions. Moreover chitosan membrane can be reused again for dialysis.

Acknowledgements

The authors would like to express our grateful thanks to the funding agencies which have been currently support to this research project as follows:

1. National Metal and Materials Technology Center (MTEC) : National Science and Technology Development Agency (NSTDA) Bangkok, Thailand.
2. The Petroleum Institute of Thailand, Bangkok, Thailand.
3. PhraUbaleegunupamajaraya, Wat Rai Khing, NakornPathom, Thailand.
4. Asian Institute of Technology (AIT) Pathumthani, Thailand.

References

1. Aiba,S.,Izume,M.,Minoura,N. and Fujiwara,Y. 1986 Preparation and properties of dialysis membranes, Chitin in Nature and Technology; Muzzarelli,R.,Jeuniaux, C. and Gooday,G.W.(eds) Plenum Press, New York.
2. ASTM 1984 Standard test methods for tensile properties of thin plastic sheeting, Designation: D 882-83.
3. ASTM 1985 Standard test methods for sulfate ions in water, Designation: E 685-88.
4. Avner,H.S. 1974 Introduction to Physical Metallurgy,2nd ed. McGraw-Hill.
5. Billmeyer,F.W.,Jr. 1984 Textbook of Polymer Science,3rd ed. John Wiley and Sons.
6. Bird,R.B.,Steward,W.E. and Lightfoot,E.N. 1960 Transport Phenomena,John Wiley and Sons, New York.
7. Chandrkrachang,S.,Chinadit,U.,Chandayot,P. and Supasiri,T. 1991 Profitable spin-offs from shrimp-seaweed polyculture,Infofish International: 6,26-28.
8. Chandrkrachang,S. 1996 Chitin and Chitosan: Multipurpose Biodegradable Biomaterials, Proceeding of MTEC annual meeting 1995, Bangkok, Thailand.
9. Chitin and Chitosan: Specialty Biopolymers for Foods, Medicine and Industry, 1989 Technical Insights, Inc.,USA.
10. Coulter,A.R. 1992 Water permeability in poly(ortho ester)s, J. Membrane Science : 65,269-275.
11. Frisch,H.L. 1978 Diffusion in inhomogeneous films and membranes, J.Membrane Science: 3,149-161.
12. Kesting,R.E. 1971 Synthetic Polymeric Membranes,McGraw-Hill,New York.
13. Kienzle-Sterzer,C.A.,Rodriguez-Sanchez,D. and Rha,C. 1982 Mechanical properties of chitosan films: effect of solvent acid,Makromol.Chem.:183,1353-1359.
14. Lapasin,R. and Pricl,S. 1995 Rheology of Industrial Polysaccharides: Theory and Application,Blackie A&P,London.
15. Muzzarelli,R.A.A. 1977 Chitin,Pergamon Press,New York.
16. Ornum,J.V. 1992 Shrimp Waste: Must it be wasted? Infofish International:6,48-52.
17. Osswald,T.A. and Menges,G. 1996 Materials Science of Polymers for Engineers , Hanser/Gardner Publications,Germany.
18. Smith,W.F. 1990 Principles of Materials Science and Engineering,2nd ed.McGraw -Hill.
19. Tadmor,Z. and Gogos,C.G. 1979 Principles of Polymer Processing,John Wiley and Sons.
20. Treatise on Analytical Chemistry Part III Analytical Chemistry of Elements Vol. 7 1961 John Wiley and Sons:103-105.
21. Williams,D.J. 1971 Polymer Science and Engineering,Prentice-Hall,USA.

CRYSTALLOSOLVATES OF β CHITIN AND ALCOHOLS

Yukie SAITO*, Takeshi OKANO*, Jean-Luc PUTAUX†, Françoise GAILL‡ and Henri CHANZY†

* *Faculty of Agriculture, the University of Tokyo, Yayoi 1-1-1, Bunkyo-ku, Tokyo 113, Japan. - E.mail: aa47086@hongo.ecc.u-tokyo.ac.jp*

† *Centre de Recherches sur les Macromolécules Végétales, CNRS, affiliated with the Joseph Fourier University of Grenoble, BP 53, 38041 Grenoble Cedex 9, France*

‡ *Laboratoire de Biologie Marine, Université Pierre et Marie Curie, 7 Quai Saint Bernard, 75252 Paris Cedex 05, France*

Abstract

Highly crystalline β chitin from the vestimentiferan tubes of *Tevnia jerichonana* formed crystallosolvates by immersion into alcohols after a swelling treatment in 7N HCl. Their crystal symmetry as well as their unit cell parameters *a*, *c* and γ generally appeared to be similar to those of the parent β chitin. However, the cell parameter *b*, which was of 0.92 nm in the anhydrous β chitin, increased steadily with the size of the alcohol, from 1.31 nm for methanol to 1.98 nm for *n*-octanol.

Keywords: β chitin, crystallosolvate, alcohol, cryo electron microscopy, X-rays.

Introduction

It was recently shown that samples of highly crystalline β chitin from the vestimentiferan tubes of *Tevnia jerichonana* could be totally decrystallized by immersion into HCl of concentration 6N and higher [1]. Crystalline chitin was recovered upon washing in water. β chitin hydrates were obtained if the strength of HCl was between 6 and 7N whereas, above this concentration, a substantial amount of α chitin was created. Full conversion of β chitin into α chitin occurred with HCl of 8N and higher. For the latter case, a solubilization of β chitin chains was implied.

In the work presented here, samples were swollen in 7N HCl and rinsed in various linear alcohols: methanol, ethanol, *n*-propanol, *n*-butanol and *n*-octanol. These samples in their alcohol environment were studied by X-ray diffraction analysis together with transmission electron cryomicroscopy.

Materials and methods

Samples of β chitin were prepared from the tubes of *Tevnia jerichonana* which had been collected in November 1987, at a depth of 2600 m, at 12°48'N 103°56'W near the East Pacific rise. The dried tubes were deproteinized by using a method described by Gaill *et al.* [2] and stored in 30% aqueous ethanol. To delaminate the tube, a weak hydrolysis was performed for 2 h in boiling 2.5N HCl. The sample was rinsed with water. In the 30% aqueous ethanol environment, the β chitin samples appeared as monohydrates whereas after the HCl boiling and subsequent washing, they were converted into the dihydrate form.

For X-ray measurements, oriented fibrous β chitin samples were prepared. After stirring the aqueous suspension during 1 h, bundles of parallel β chitin fibrils were obtained. The specimens were rinsed in water, treated in 7N aqueous HCl for 30 min, blotted between filter papers and immersed, at room temperature, into dry alcohols (methanol, ethanol, *n*-propanol, *n*-butanol, *n*-pentanol or *n*-octanol). Then, they were briefly pressed between filter papers and immediately sealed in glass capillaries before evaporation of the alcohol. The specimens were mounted in a flat-film vacuum camera and X-rayed. The diffractograms recorded on a Fuji imaging plate were calibrated with reflections of NaF (characteristic spacing: 0.2319 nm) dusted directly onto the specimens.

Samples of chitin-methanol complexes were also prepared for cryo transmission electron microscopy. One drop of the concentrated aqueous chitin suspension was dispersed into a few ml of 7N HCl. After 30 min, the sample was centrifuged and rinsed in methanol. Cryomicroscopy specimens were prepared using the technique described in [3]. A liquid film of the suspension was fast frozen in liquid propane cooled down to liquid nitrogen temperature. The frozen samples were transferred into the microscope at liquid nitrogen temperature and observed in a Gatan cryo-holder, using a Philips CM200 Cryo microscope, operated under low dose conditions at 80 kV for imaging purpose and 200 kV for selected area electron diffraction.

Results and discussion

Figure 1a is an X-ray diffractogram of β chitin washed in methanol after a 7N HCl treatment. The rings in the diagram are

sharp and suggest that the sample had a high crystallinity. After calibration, the unit cell parameters were calculated to be a=0.465 nm, b=1.310 nm, c=1.037 nm (chain axis) and γ=93.1° (see Table 1). The absence of 001 and 003 reflections indicates that the unit cell of the sample most likely had a $P2_1$ symmetry. In fact, the diagram in Figure 1a can be indexed along a monoclinic unit cell which is similar to that of anhydrous β chitin except for the b parameter, which is 38% larger. This suggests that methanol molecules became intercalated inside the β chitin unit cell during the washing step to give a chitin-methanol crystallosolvate. After evaporation of the methanol at 60°C, the diffractogram of anhydrous β chitin was restored with a shorter d_{010} of 0.910 nm (Fig.1b). Thus, the methanol that was in the crystallosolvate had a substantial mobility.

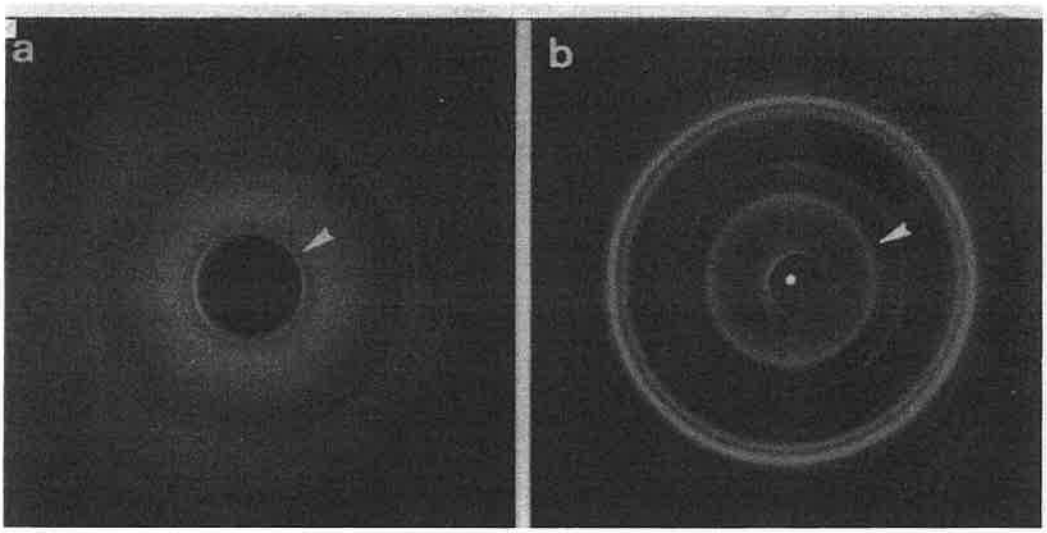

Figure 1: X-ray diffractograms - **a)** *T. jerichonana* β chitin-methanol crystallosolvate, with d_{010} = 1.31 nm (arrow). **b)** same sample as a) but after evaporation of the methanol, with d_{010} = 0.91 nm (arrow).

Table 1: d-spacings of the β chitin-methanol crystallosolvate.

indices	d_{obs} (nm)	d_{cal} (nm)
1 0 0	0.472	0.465
1 1 0	0.424	0.431
1-1 0	0.446	0.446
1-2 0	0.385	0.389
0 1 0	1.309	1.308
0 0 1	1.036	1.037
0 1 3	0.339	0.334

The β chitin-methanol crystallosolvate was also visualized using cryo electron microscopy. Figure 2 shows some microfibrils which are embedded in a film of vitreous methanol at liquid N_2 temperature. The microfibrils have parallel edges with a lateral size ranging from 30 to 80 nm and a shape which remained similar to the one observed before treatment in HCl. Quite interestingly, each fiber is clearly fibrillated into an assembly of parallel sub-fibrils less than 5 nm in width. Such a fibrillation must be formed during the 7N HCl treatment. However, it seems that the parallel arrangement of chitin chains inside each sub-fibril is preserved. Electron diffractograms were recorded on individual microfibrils (Fig.2b). In most patterns, each layer line exhibits some streaks parallel to the equator line, probably due to the fibrillation along the fiber axis [4]. The equatorial spots are discrete and correspond to the *d*-spacings 1.31 and 0.47 nm. These values could also be measured from the X-ray pattern in Figure 1a.

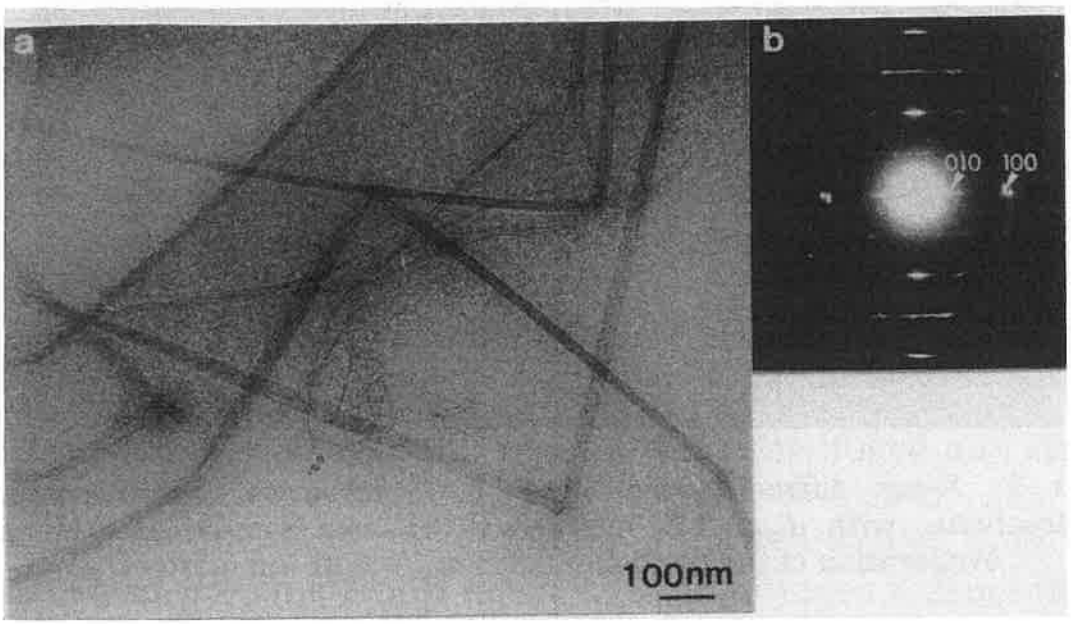

Figure 2: **a)** electron micrograph of the *Tevnia* β chitin-methanol crystallosolvate embedded in vitreous methanol and observed at liquid nitrogen temperature. **b)** electron diffraction pattern recorded on a microfibril bundle with vertical axis.

With the other linear alcohols, X-ray diffractograms different from the original β chitin were also observed. The unit cell parameters measured from the *d*-spacings are given in Table 2. Remarkably, for all alcohols, the unit cell was expanded along the

As the inter-chain distance along the amide hydrogen bond direction was rather stable for most crystallosolvate, it is suggested that the sheet-like structure of chitin is maintained in 7N HCl. It is worth mentioning that such a sheet-like structure and its susceptibility toward swelling in alcohol is not limited to chitin. In a related case, alkali-swollen cellulose can also form similar crystallosolvates with water, methanol, ethanol, *n*-propanol and *n*-butanol [5].

Conclusion

Crystallosolvates of β chitin and various alcohols were formed by washing 7N HCl-swollen β chitin samples in alcohols. In most cases, these crystals had monoclinic unit cells with parameters generally similar to those of β chitin, except for a larger *b*. This expansion which mainly occurred along this direction suggests a sheet-like arrangement of the chitin chains in the β chitin crystal as well as in the β chitin-alcohol crystallosolvates.

References

[1] Saito, Y., Putaux, J.-L., Okano, T., Gaill, F. and Chanzy, H., *Macromolecules* 1997; 30: 3867.

[2] Gaill F., Persson J., Sugiyama J., Vuong R. and Chanzy H., *J. Struct. Biol.* 1992; 109: 116.

[3] Sugiyama, J., Rochas, C., Turquois, T., Taravel, F. and Chanzy, H., *Carbohydr. Polym.* 1994; 23: 261.

[4] Tadokoro H., in *Structure of Crystalline Polymers*, John Willey & Sons, New York, 1979, p.150.

[5] Warwicker, J. O. and Wright A. C., *J. Appl. Polym. Sci.* 1967; 11: 659.

Acknowledgments

Y. Saito acknowledges the support of CERMAV-CNRS for a 16 month fellowship and the Japan Society for the Promotion of Science (JSPS) for a two year fellowship.

ADSORPTION BEHAVIOR OF GERMANIUM(IV) ON N-2,3-DIHYDROXYPROPYL CHITOSAN RESIN

Yoshinari INUKAI, Yasuhiko KAIDA and Seiji YASUDA,

Kyushu National Industrial Research Institute, 807-1 Shuku-machi, Tosu, Saga 841, (JAPAN). Fax: +81 942 83 0850 E. Mail: inukai@kniri.go.jp

Abstract

N-2,3-Dihydroxypropyl chitosan resin, prepared from chitosan and a 1,2-diol, adsorbed only germanium(IV) from aqueous solutions containing semimetals over the range of acidic to weakly basic media. The adsorption capacities of the chitosan resin were up to about 1.4 mmol g^{-1}. The selective separation of germanium(IV) from tellurium(VI) and boron was achieved with a column method using the chitosan resin. The breakthrough points of germanium(IV) in the chitosan resin column were about 90 bed volumes in weakly basic media. The germanium(IV), adsorbed on the column, was quantitatively recovered by elution with hydrochloric acid.

Keywords: Germanium(IV), N-2,3-dihydroxypropyl chitosan, chitosan, tellurium(VI), boron

In previous studies we synthesized branched-saccharide chitosan resins[1,2] and 1,2-diol-type polystyrene resins[3,4] to obtain novel adsorbents with high selectivity for semimetals. The branched-saccharide chitosan and 1,2-diol-type polystyrene resins selectively adsorbed germanium(IV) from aqueous solutions containing semimetals by a batch method. The branched-saccharide chitosan resins had larger adsorption capacities than the 1,2-diol-type polystyrene resins. By a column method, however, the branched-saccharide chitosan resins adsorbed both germanium(IV) and boron, and the 1,2-diol-type polystyrene resins adsorbed germanium(IV), boron and tellurium(VI).

In the present study we synthesized N-2,3-dihydroxypropyl, 1,2-diol-type, chitosan resin to obtain a novel adsorbent with high selectivity for germanium(IV), and investigated the adsorption behavior of germanium(IV), tellurium(VI) and boron on the chitosan resin by batch and column methods.

Materials and methods

Materials

Chitosan (trade name: Chitosan 10B, deacetylated degree 100 %) was produced by Katokichi Co., Ltd., Japan. Chitosan beads (trade name: Chitopearl "Basic" AL-03, particle size 0.3 mm in diameter) were produced for the crosslinking of chitosan particles with ethylene glycol diglycidyl ether by Fuji Spinning Co., Ltd.,

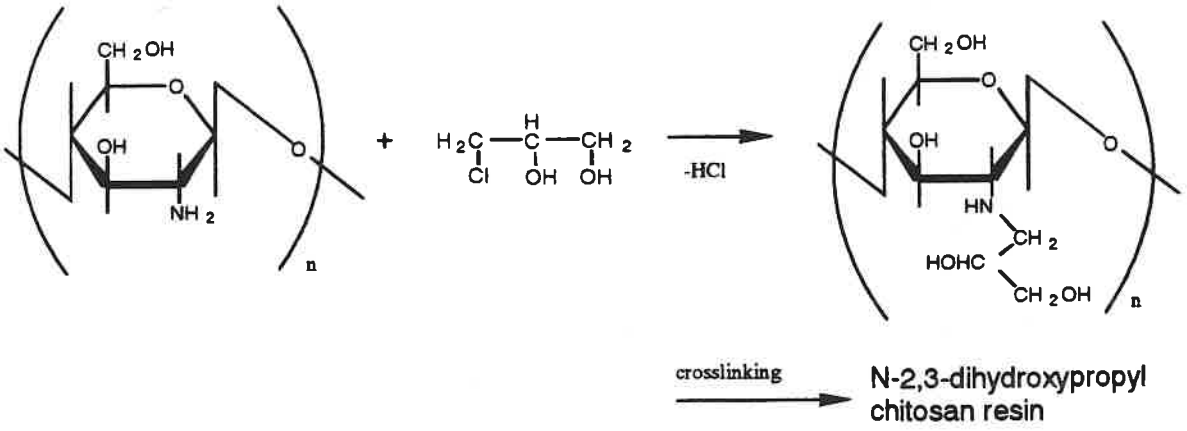

Scheme 1 Synthesis of N-2,3-dihydroxypropyl chitosan resin.

Japan.[5] Other reagents were reagent or higher grade, and were used without further purifications. All of the aqueous solutions were prepared with distilled and deionized water.

Preparation

N-2,3-Dihydroxypropyl chitosan resin was prepared from chitosan and 3-chloro-1,2-propanediol, as shown in Scheme 1. Sodium hydroxide (4.03 g) in methanol (120 cm^3) was added to a mixture of chitosan (5.00 g) and 3-chloro-1,2-propanediol (15.08 g) in dioxane (120 cm^3), and the mixture was heated at 60-70℃ for 24 h with stirring. The resulting gel was filtered and washed with deionized water and methanol. The most part (5.15 g) of the dried gel (5.66 g) was, then, successively crosslinked by chloromethyloxirane (4.01 g) at 60-70℃ for 5 h in 0.1 mol dm^{-3} sodium hydroxide solution (100 cm^3). The product was filtered and washed with diluted hydrochloric acid, successively deionized water and methanol, to give dried N-2,3-dihydroxypropyl chitosan resin (6.08 g). Also, similar reaction of the original chitosan beads with 3-chloro-1,2-propanediol was carried out at 60-70℃ for 24 h in the presence of sodium hydroxide, and gave N-2,3-dihydroxypropyl chitosan beads. The introduction of 2,3-dihydroxypropyl group into chitosan and the original chitosan beads was confirmed by the increases in the atomic ratios of carbon to nitrogen of the N-2,3-dihydroxypropyl chitosan resin and beads, compared with those of chitosan and the original chitosan beads, respectively.

Batch method procedure

About 50 mg of the dried N-2,3-dihydroxypropyl chitosan resin or beads and 25 cm^3 of a semimetal sample solution were shaken for 24 h in a screwed vial maintained at 25℃. The initial concentration of semimetal in the sample solution was about 10 mmol dm^{-3}, and 0.1 mol dm^{-3} potassium chloride solution was used to maintain a constant ionic strength of the sample solution. The initial pH was adjusted with addition of 0.1-0.5 cm^3 diluted hydrochloric acid or aqueous sodium hydroxide. In experiments of the competitive adsorption of semimetals, ammonium chloride - ammonia buffer was used as the sample solution to maintain

a constant pH value. The amounts of adsorbed semimetals were calculated from the differences between the concentrations of semimetals in the aqueous solutions before and after the adsorption, and expressed as mmol per g of the chitosan resin or beads. The concentrations of semimetals were determined using an inductively coupled plasma (ICP) atomic-emission spectrometer (Seiko Instruments Inc., Japan; Model SPS 1200AR). The pH values at equilibrium after 24 h were measured with a pH meter (Horiba, Ltd., Japan; Model F-22).

Column method procedure

The sample solution, containing semimetals, such as germanium(IV), tellurium(VI) and boron, was loaded on a column (5 mm in diameter), packed with about 1.4 cm^3 of the wet N-2,3-dihydroxypropyl chitosan resin, at a flow rate of space velocity (SV) about 10 h^{-1} at room temperature. The concentration of semimetals in the sample solution was about 1 mmol dm^{-3}. An ammonium chloride - ammonia buffer was used as the sample solution to maintain a constant pH value. The elution of the column was carried out by 1 mol dm^{-3} hydrochloric acid at a flow rate of SV about 10 h^{-1}.

In recycle experiments, 111 bed volumes of 1 mmol dm^{-3} germanium(IV) solution, adjusted with a buffer to pH 8.2, were loaded on the N-2,3-dihydroxypropyl chitosan resin column at a flow rate of SV about 10 h^{-1} at room temperature in each cycle. After being washed with deionized water, germanium(IV) in the column was eluted with 37 bed volumes of 3 mol dm^{-3} hydrochloric acid at a flow rate of SV about 10 h^{-1}. The column was reused after being washed with 1 mol dm^{-3} sodium hydroxide solution and deionized water in recycle experiments. The recovery of germanium(IV) was calculated from the ratio of the amount eluted with the eluent to the amount adsorbed on the column.

Results and discussions

Effect of pH on the adsorption of semimetals on N-2,3-dihydroxypropyl chitosan resin

Figure 1 shows the effect of pH on the adsorption of germanium(IV), tellurium(VI) and boron on N-2,3-dihydroxypropyl chitosan resin. The pH values in Fig.1 were obtained at equilibrium after 24 h. The adsorption of germanium(IV) had a maximum value (ca. 1.4 mmol g^{-1}) at around pH 4. The adsorption capacities of the chitosan resin for germanium(IV) were large over the range of acidic to weakly basic media, but were smaller than those of the branched-saccharide

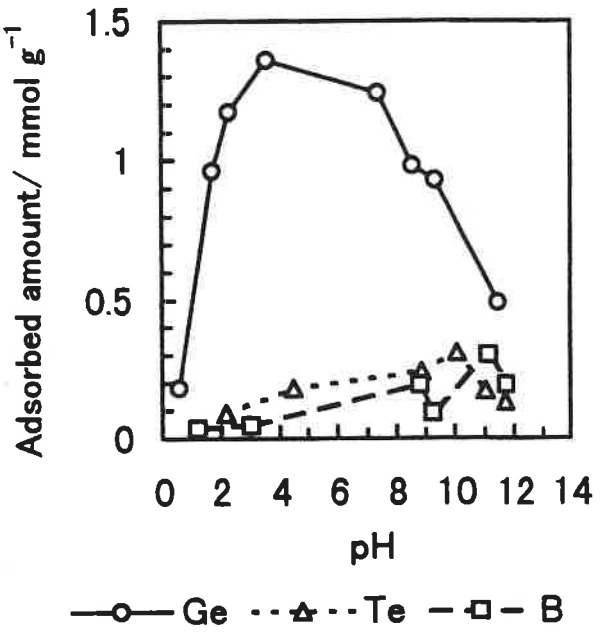

Fig. 1 Effect of pH on the resin

Table 1
Separation factors of germanium(IV) to the other semimetals for the competitive adsorption of semimetals on N-2,3-dihydroxypropyl chitosan resin and beads

Chitosan resin[a] and beads[b]	Separation factor (pH[c])				
	Ge(IV) Te(VI)	Ge(IV) B(III)	Ge(IV) As(III)	Ge(IV) As(V)	Ge(IV) Se(VI)
resin[a]	2.6 (6.8)	14 (8.5)[d]	8.9 (8.5)[d]	230 (8.3)[d]	18 (8.4)[d]
beads[b]	4.2 (8.0)	8.1 (8.4)[d]			180 (8.2)[d]

[a]2,3-Dihydroxypropyl group was introduced into chitosan.
[b]2,3-Dihydroxypropyl group was introduced into chitosan beads.
[c]Equilibrium pH.
[d]Buffer solution was used.

chitosan resins.[1] In strongly acidic and strongly basic media, only a small amount of germanium(IV) was adsorbed on the chitosan resin. In contrast to the cases of the branched-saccharide chitosan[1,2] and 1,2-diol-type polystyrene[3,4] resins, tellurium(VI) and boron were hardly adsorbed on the chitosan resin over the whole pH range.

Separation factors of germanium(IV) to the other semimetals for the competitive adsorption of semimetals on N-2,3-dihydroxypropyl chitosan resin and beads

The competitive adsorption experiments of semimetals on N-2,3-dihydroxypropyl chitosan resin and beads were carried out to obtain the separation factors of germanium(IV) to the other semimetals. Table 1 shows the representative results at an equilibrium pH of 6.8-8.5. This pH range was selected to avoid the adsorption of other metals on polyhydroxy compounds in acidic media.[6] The separation factor (α) is defined as $\alpha = K_{d1} / K_{d2}$, where K_{d1} and K_{d2} represent the distribution coefficient [the semimetal concentration on the chitosan resin (mg kg^{-1}) / that in the aqueous solution (mg dm^{-3}) after the adsorption] of germanium(IV) and the other semimetal, respectively. Separation factors of germanium(IV) to tellurium(VI), boron, arsenic(III), arsenic(V), selenium(IV) and selenium(VI) were much larger. That is, few amounts of tellurium(VI), boron , arsenic(III), arsenic(V), selenium(IV) and selenium(VI) were adsorbed on the chitosan resin and beads due to the competitive adsorption with germanium(IV). Consequently, the chitosan resin and beads were found to be highly selective adsorbents for germanium(IV).

Adsorption behavior of semimetals on the N-2,3-dihydroxypropyl chitosan resin column

Figure 2 shows breakthrough curves for germanium(IV), tellurium(VI) and boron in the N-2,3-dihydroxypropyl chitosan resin column at pH 8.4. Tellurium(VI) and boron leaked immediately, as predicted from Fig. 1, and the concentrations of tellurium(VI) and boron in the effluent fractions rapidly reached

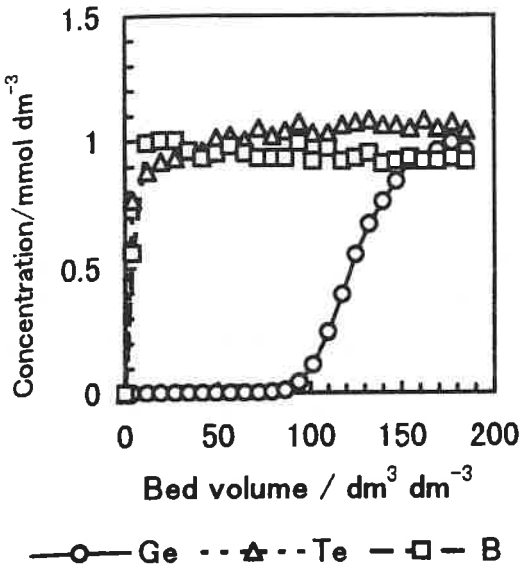

Fig. 2 Breakthrough curves

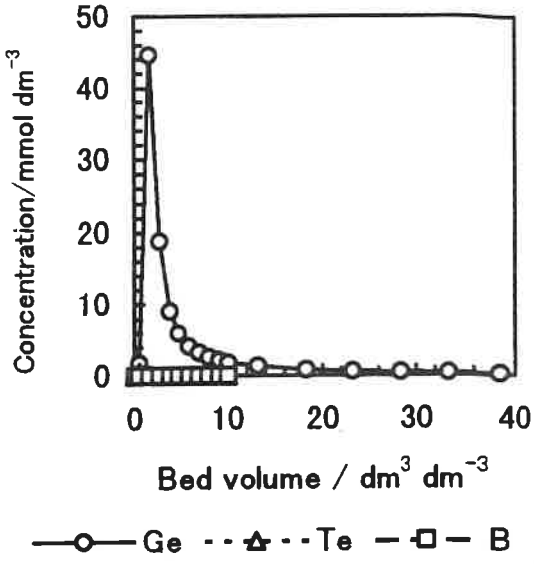

Fig. 3 Elution curves

Table 2
Elution of germanium(IV) adsorbed on N-2,3-dihidroxypropyl chitosan resin with hydrochloric acid

Cycle No.	Ge(IV) adsorbed[a] / mg	Ge(IV) eluted[b] / mg	Recovery / %
1	11.32	11.13	98.3
2	11.30	11.32	100
3	10.90	10.58	97.0

[a]Sample volume was 111 bed volume of 1 mmol dm^{-3} germanium(IV) buffer solution at pH 8.2.
[b]Eluent volume was 37 bed volume of 3 mol dm^{-3} hydrochloric acid.

the initial concentrations. Germanium(IV) was adsorbed on the column; the breakthrough point of germanium(IV) was 85 bed volumes.

Figure 3 shows the elution curves for germanium(IV), tellurium(VI) and boron with 1 mol dm^{-3} hydrochloric acid in the N-2,3-dihydroxypropyl chitosan resin column. Since no tellurium(VI) and boron were adsorbed on the column, they were not eluted. Most of germanium(IV) was eluted in the initial 10 bed volumes of the effluent.

The cycle of adsorption, washing, elution and washing steps was repeated 3 times in order to check the reproducibility of the chitosan resin column system in the adsorption and desorption of germanium(IV). The results are shown in Table 2. The germanium(IV), adsorbed on the column, was quantitatively eluted with hydrochloric acid in each cycle. That is, selective separation and a considerable

concentration effect of germanium(IV) were achieved by utilizing the chitosan resin column.

Conclusion

N-2,3-Dihydroxypropyl chitosan resin, prepared from chitosan and a 1,2-diol, adsorbed only germanium(IV) from aqueous solutions containing semimetals. The selective separation of germanium(IV) from tellurium(VI) and boron was achieved with a column method using the chitosan resin. The germanium(IV), adsorbed on the column, was quantitatively recovered by elution with hydrochloric acid.

References

1) Y. Inukai, Y. Kaida and S. Yasuda, *Anal. Chim. Acta*, **343**, 275 (1997).
2) Y. Inukai, Y. Kaida and S. Yasuda, *Abstracts of Papers, ASIANALYSIS IV*, Fukuoka, May 1997, 1P40.
3) S. Yasuda, Y. Inukai and H. Ohba, *Bunseki Kagaku*, **42**, 713 (1993).
4) S. Yasuda, Y. Inukai and H. Ohba, *Nippon Kagaku Kaishi*, **1994**, 221.
5) Y. Kawamura, M. Mitsuhashi, H. Tanibe and H. Yoshida, *Ind. Eng. Chem. Res.*, **32**, 386 (1993).
6) S. Yasuda and K. Kawazu, *Bunseki Kagaku*, **37**, T67 (1988).

Acknowledgements

We thank Mr. Toyotaka Chinen for his experimental help and Professor Toshio Matsuda (Tohwa University) for his helpful discussions.

PIPEMIDIC ACID - LOADED CHITOSAN MICROSPHERES PRODUCED BY THE SPRAY-DRYING METHOD

Mateja BURJAK, Marija BOGATAJ and Aleš MRHAR
Faculty of Pharmacy, University of Ljubljana, Aškerčeva 7, 1000 Ljubljana, Slovenia

Abstract
Chitosan in the form of hydrochloride, dissolved in purified water and pipemidic acid as hydrophilic model drug, dissolved in 0.01 M NaOH, were employed in the study. Different volumes of the drug solution were added to the solution of polymer to obtain microspheres with different drug content by the use of spray-dryer.
Chitosan microspheres so prepared had an oval shape, particles with mean diameter 3.5 μm, encapsulation efficiency falling from 104 % at 5 % of the income drug to 86.5 % at 35 % of the income drug, yield of production falling from 36.7 % at pump setting 2 to 16.4 % at 12 and rapid release of the drug.

Keywords
microspheres; spray-drying; chitosan; pipemidic acid; particles characteristics: morphology, size; spray-drying: encapsulation efficiency, yield of production; pipemidic acid dissolution.

Introduction

Spray-drying appears to be an attractive technique as it is one step, fast method, suitable for heat sensitive drugs. Among other techniques it is used for the preparation of microparticulate drug delivery systems such as microspheres which are obtained by spraying a solution of drug and polymer. The process involves assessing of technological parameters such as: concentration of the polymer and the drug in the solution to be sprayed, inlet and outlet air temperatures, spray flow, pump setting, heating and exhausting (1).
Chitosan, a cationic polyelectrolyte obtained by chitin alkaline hydrolysis is a hydrophilic, positively charged polysaccharide and appears to be a suitable material both for control of release kinetics and for targeting of therapeutic agents. It exhibits biocompatibility, biodegradability, bioadhesive properties and affinity for specific cells (2).
The aim of this study is to formulate hydrophilic pipemidic acid loaded chitosan microspheres utilizing water medium and to study the effect of various experimental conditions on size and shape of particles, yield of production, encapsulation efficiency and drug release.

Materials and methods

Materials
Pipemidic acid as a model drug was supplied by Lek, Ljubljana, Slovenia. Chitosan hydrochloride (Protasan CL 210) was purchased from Pronova ®, Oslo, Norway. Degree of deacetylation was 73%. Other substances and solvents were all of analytical grade.
Preparation of microspheres
Microspheres preparation was performed by spray-drying with apparatus Mini Büchi 190 (Büchi Laboratoriums-Technik AG, Flawil, Switzerland). Chitosan microspheres with different contents of pipemidic acid (5, 15, 25, and 35 w/w%, samples S1-S19) (Table 1), were prepared. The drug was dissolved in 0.01 M NaOH (0.22 w/w%) and the polymer in purified water (1 w/w%). Different volumes of drug solution were added slowly with

stirring to the solution of polymer to get the microspheres with different drug content. The spray-drying conditions were set up as follows: inlet temperature, 110 °C; pump setting, 2-12; aspirator setting, 7; spray flow, 500 NL/h. Drug-free microspheres (sample S0) were also prepared under the same spray-drying conditions. Additionally, flows of solutions were measured for samples S7-S15.

Microspheres evaluation

Surface characteristics were examined by means of a scanning electron microscope (SEM). The microspheres were coated with C + Au/Pd using a vacuum evaporator (Jeol). Samples were examined with a scanning electron microscope (Jeol SM2) at accelerating voltage 10 kV using a secondary electron technique. Tilt was 45 ° and working distance 12 mm.

Yields of production, expressed as the weight percent of product obtained with respect to the initial weight of polymer and drug, were determined by weighing of microspheres after they have been kept at room temperature under reduced pressure overnight.

Drug content was determined by dissolving the microspheres in 0.1 M HCl and analysing the pipemidic acid by UV derivative spectrophotometry.

Dissolution tests were carried out in USP XXIII dissolution apparatus 2 (paddle method), using a Tyrode solution as dissolution medium. Stirring rate was maintained at 100 rpm and temperature at 37 °C. The samples were assayed by UV derivative spectrophotometry (UV spectrophotometer Perkin Elmer Lambda 15).

The solubility of pipemidic acid was tested in different media: 0.1 M HCl, 0.001 M HCl, 0.001 M NaOH and 0.01 M NaOH. On the basis of solubility results the solution of the drug in 0.01 M NaOH was prepared, spray-dried under the same experimental conditions as microspheres and the dissolution of the product was evaluated. These results were compared with the dissolution results of unsprayed pipemidic acid and the results on release of the drug from the microspheres.

Results and discussion

Results of microsphere characterisation by SEM are shown in Figures 1, 2 and 3.

In the case of drug free microspheres (Figure 1), the surfaces were very smooth and the shape of these microspheres was rather oval than spherical. Particle sizes range from 0.5 to 15 μm, most of them were around 3.5 μm. SEM performed on batches S11 and S15 (Figure 2), obtained by spraying chitosan solutions with different concentrations of drug, shows that this parameter affects greatly microsphere formation. With the increasing amount of the incorporating drug erythrocyte-shaped particles occurred. No changes in particle size are detectable changing the income share of the drug. We assume that the larger amount of the drug probably lowers the permeability of the crust that occurs during the drying of drops. Drying is obstructed and consequently particles break because of increased internal pressure. Batches S14 and S9 (Figure 3) were prepared under the same experimental conditions except solution flow. From this figure it can be seen that less erythrocyte-shaped particles occur and some of them were fused at higher solution flow.

The microspheres were of an oval shape whether they were drug loaded or not. The mean diameters of drug-loaded microspheres are generally smaller than those without incorporated drug.

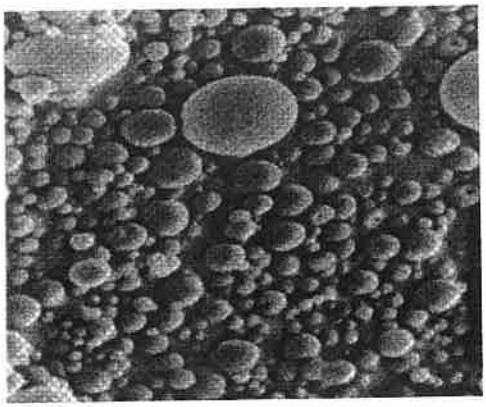

Figure 1. SEM photomicrograph of drug-free microspheres (S0).

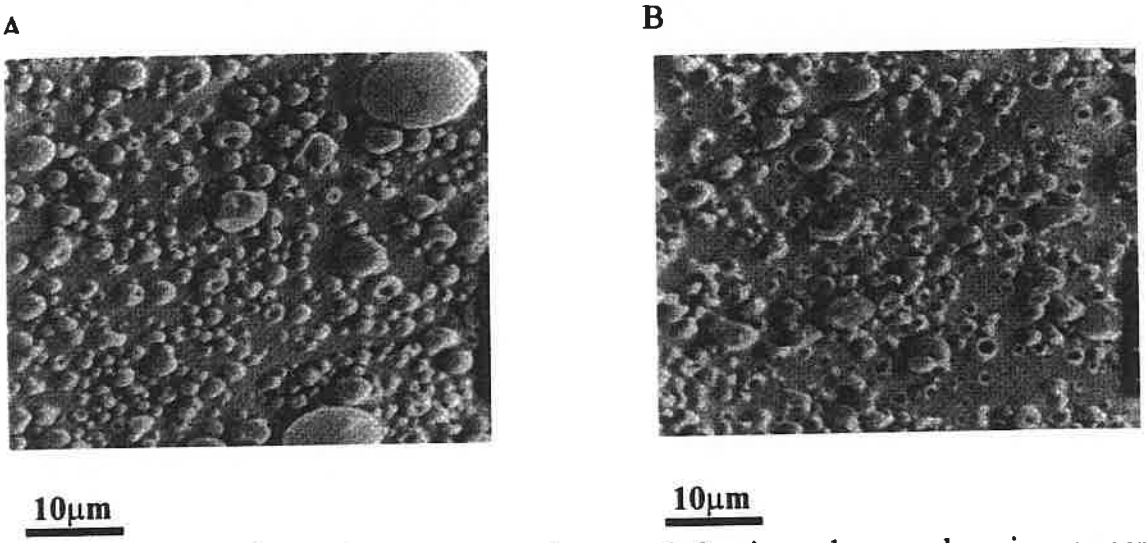

Figure 2. SEM photomicrographs of drug-loaded microspheres; changing experimental parameter was drug content. A: 5.2 % (S11); B: 24.5 % (S15).

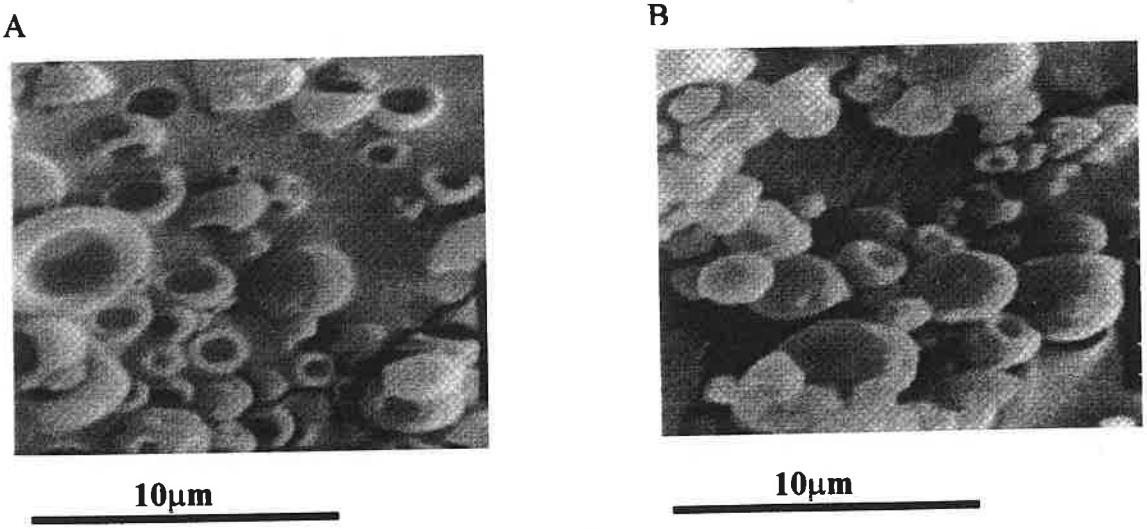

Figure 3. SEM photomicrographs of drug loaded microspheres; changing experimental parameter was solution flow. A: 4.4 ml/min (S14); B: 8.8 ml/min (S9).

The influence of solution flow on the outlet temperature and the yield of production was followed as well (samples S9, S14 and S19). Increase of solution flow leads to the decrease of yield and also to the decrease of outlet temperature. Yield of production falls from 36.7 % at solution flow 4.4 ml/min to 16.4 % at 14.8 ml/min and linear relationship between solution flow and yield of production can be seen.
The yields of the spray-drying procedure were 36.7 % or less (Table 1). Low yields were the consequence of several reasons. A considerable amount of the microspheres was always found to leave the apparatus with the air flow and large amount also adhered on other apparatus elements than the collector. Bitz et al. (3) suggested the possibility to increase the yield. That would be to increase the concentration of the spray-drying solution, but as the solution concentration also strongly influences the shape of the microspheres, modifications of this parameter are restricted within very narrow limits. Moreover, in our systems high concentrations can not be used due to precipitation of chitosan in concentrated solutions.

Table 1. Variable process conditions and product yields of the spray-dried microspheres with different pipemidic acid shares.

Sample	income share of pipemidic acid (%)	pump setting	solution flow (ml/min)	outlet temperature (°C)	yield of production (%)
S0	0	6		85-87	28,3
S1	5	6		69-71	29,6
S2	15	6		65-67	30,9
S3	25	6		62-63	29,3
S4	25	6		61-62	28,8
S5	35	6		59-60	29,1
S6	45*	/	/	/	/
S7	5	6	7,3	65-66	27,8
S8	15	6	8,3	62-63	24,2
S9	25	6	8,8	60-61	24,9
S10	35	6	8,8	60-61	24,4
S11	5	6	6,5	66-67	26,9
S12	15	5	6,5	65-66	34,9
S13	25	2	4,2	75-76	34,5
S14	25	2	4,4	75-76	36,7
S15	25	4	6,4	66-67	33,8
S16	25	4	6,5	66-67	/
S17	25	6	8,8	60-61	26,5
S18	25	12	14,4	44-45	17,9
S19	25	12	14,8	46-47	16,4

* Microspheres with 45 % of the income drug can not be prepared due to precipitation of chitosan in the spray-drying solution.

Each process variable has a significant effect on product characteristics, which in turn affects the release of the drug. Such knowledge will help the formulator to choose the

optimal conditions for preparing dosage form with a predictable release pattern. Varying the drug/polymer ratio is a fundamental requirement for optimising the preparation of products with controlled release rates (4). In our experiments 5, 15, 25 and 35 % of pipemidic acid were used for incorporation in microspheres. From Figure 4 it can be seen that encapsulation efficiency is influenced by income share of pipemidic acid and falls from 104 % at 5 % of the income drug to 86.5 % at 35% of the income drug.

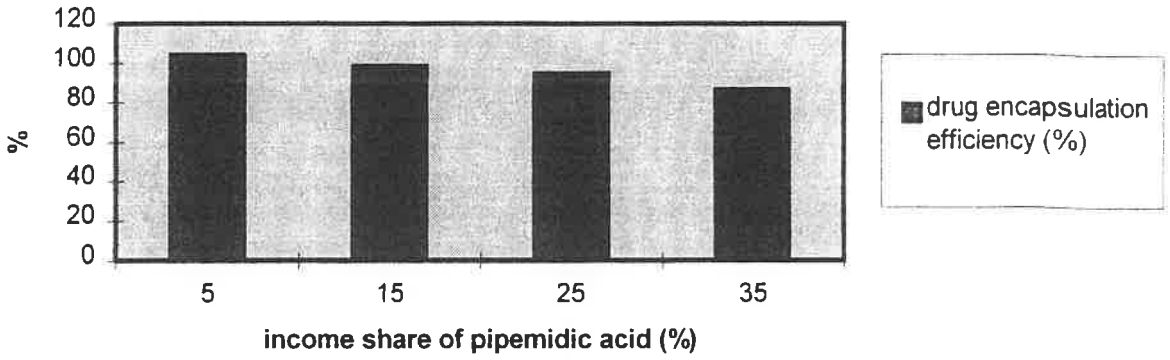

Figure 4. The influence of the income share of pipemidic acid on the drug encapsulation efficiency.

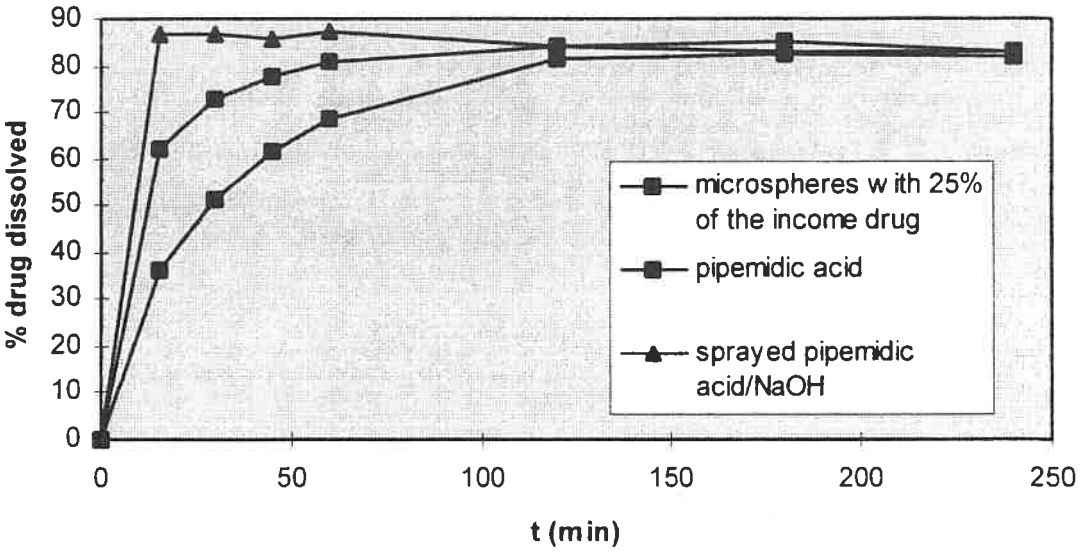

Figure 5. Dissolution behaviour of pipemidic acid loaded chitosan microspheres, of unsprayed pipemidic acid and spray-dried pipemidic acid from 0.01 M NaOH solution.

On the basis of the experimental results, authors (5) concluded that dissolution profiles of spray-dried product are dependent on the type of polymer and its hydrophilicity. It is possible to improve the dissolution rate of poorly soluble drugs by microencapsulation with hydrophilic polymers. Chitosan has been used as vehicle for sustained release of drugs as well as enhancer of dissolution rate of water-insoluble drugs (6). He et al. (7) studied the release rate of cimetidine and famotidine from chitosan spray-dried microspheres. The

results showed that cimetidine rapidly released from the microspheres and most of it was dissolved in few minutes. When famotidine was used, the release rate was retained.
Pipemidic acid dissolution data obtained by USP method are shown in Figure 5. Product obtained by spray-drying the drug solution in 0.01 M NaOH, dissolved in few minutes. Most of the drug was released during the first 15 minutes from the microspheres with 25% of the income drug (average profile of samples S3, S4, S9 and S13-S19). This is most likely due to the small size and porous morphology of microspheres. Additionally, hydrophilic nature of the polymer and the drug which both have high affinity for water contributes to fast release of the drug. By comparing this data with dissolution data of unsprayed pipemidic acid the slowest dissolution of the pure drug was observed. Rapid release from microspheres and fast dissolution of sprayed pipemidic acid could be also the consequence of formation of sodium salt of pipemidic acid and/or its transformation to amorphous form. The experimental conditions which were changed during the study have no influence on drug release from microspheres.

Conclusions

Spray-dried pipemidic acid loaded chitosan microspheres were prepared and evaluated. On the basis of the results the following conclusions can be drawn:

- the aqueous solutions for preparation of pipemidic acid / chitosan microspheres should be obtained "in situ",
- the surfaces of prepared microspheres were smooth and the shape was oval, particle sizes range from 0.5 to 15 μm; the increasing amount of the drug caused more erythrocyte-shaped particles; pump setting (solution flow) showed the influence on microspheres shape and the yield of production,
- with the increasing share of the income drug, the drug encapsulation efficiency decreased,
- pipemidic acid release from the microspheres was very fast,
- the prepared microspheres are intended to be used as mucoadhesive drug delivery system.

References

1. Conte, U., Conti, B., Giunchedi, P. and Maggi, L. Drug Dev. Ind. Pharm. 1994, 20 (3), 235
2. Orienti, I., Aiedeh, K., Gianasi, E. and Bertasi, V. J. Microencapsul. 1996, 13 (4), 463
3. Bitz, C. and Doelker, E. Int. J. Pharm. 1996, 131, 171
4. Giunchedi, P. and Conte, U. S.T.P. Pharma. Sciences 1995, 5 (4), 276
5. Wan, L.S.C., Heng, P.W.S. and Chia, C.G.H. Drug Dev. Ind. Pharm. 1992, 18 (9), 997
6. Amadóttir, S.G. and Kristmundsdóttir, T. Eur. J. Pharm. Sci. 1996, 4, S 134
7. He, P., Davis, S.S. and Illum, L. Eur. J. Pharm. Sci. 1996, 4, S 173

Polynucleotide-Chitosan Complex, an Insoluble but Reactive Form of Polynucleotide

Hikoya HAYATSU[a], Takashi KUBO[a], Yuji TANAKA[a] and Kazuo NEGISHI[b]

Faculty of Pharmaceutical Sciences[a], Gene Research Center[b], Okayama University, Tsushima, Okayama 700, Japan ([a]Fax: 81-86-251-7927 E Mail: hayatsu@ph2ews1.okayama-u.ac.jp)

DNA formed an insoluble complex on mixing with chitosan (poly-D-glucosamine) in solution. DNA content in the complex was about 50% (w/w). The DNA stayed insoluble in aqueous media of pH 2-7; e.g., on treatment of the DNA-chitosan complex with phosphate-buffered saline at pH 7 and 37°C for 26 h, DNA released into the aqueous phase was less than 0.05%. Obviously, DNA and chitosan formed a tight complex due to ionic interactions. The DNA can be solubilized by treatment with 0.1 N NaOH. RNA and other polynucleotides formed similar insoluble complexes with chitosan. The DNA on chitosan can be digested with nucleases, and can be chamically modified. Using polynucleotide-chitosan as an adsorbent, affinities of reagents to polynucleotides can be determined directly. With this technique it was found that carcinogenic heterocyclic amines have affinity to RNA as well as to DNA. These results suggest that the polynucleotides in the chitosan complex were accessible by enzymes and reagents.

Keywords: DNA-chitosan complex, RNA-chitosan complex, Bisulfite modification of DNA-chitosan, Enzymatic reaction on DNA in DNA-chitosan, Heterocyclic amine binding to polynucleotides

Abbreviations used: Glu-P-1, 2-amino-6-methyldipyrido[1,2-*a*:3',2'-*d*]imidazole; IQ, 2-amino-3-methylimidazo[4,5-*f*]quinoline; MeIQx, 2-amino-3,8-dimethylimidazo[4,5-*f*]quinoxaline; PhIP, 2-amino-1-methyl-6-phenylimidazo[4,5-*b*]pyridine; Trp-P-2, 3-amino-1-methyl-5H-pyrido[4,3-*b*]indole

---

We report here that, by mixing chitosan and DNA solutions, a precipitate of the DNA-chitosan complex is formed in which the DNA content is as high as 50% and yet the complex is insoluble in aqueous media over a wide range of pH values. RNA and other polynucleotides also formed similar complexes. The DNA in the chitosan complex was accessible to reagents and enzymes. Thus,

the DNA on chitosan can be chemically modified and agents such as ethidium bromide and carcinogenic heterocyclic amines can bind to polynucleotides in the chitosan complex. DNA attached to chitosan can be attacked by nucleases.

Materials and Methods

Preparation of DNA-chitosan and other polynucleotide-chitosans A phosphate-buffered saline solution (PBS; 10 mM Na phosphate, pH 7.2, 0.15 M NaCl) of DNA or other polynucleotides (10 mg in 10 ml) was cooled in ice and stirred mechanically. To it was added dropwise a cold solution of chitosan (Wako Chemicals, Tokyo: 30 mg in 10 ml; prepared by neutralizing slowly a solution of chitosan in 0.05 N HCl with 0.025 N NaOH to pH 5). A fibrous precipitate was immediately formed, and the mixture was allowed to stand in the ice for 0.5 h. The precipitate was collected by centrifugation and washed three times with 20 ml PBS, then with water (10 ml), ethanol and diethyl ether, and dried. From DNA, a 10-20 mg complex was obtained. As judged from the absorbance of the supernatants of the reaction mixture and the washings, about 95% of DNA used was precipitated (see Table 1). From heat-denatured DNA and other polynucleotides, similar precipitates were obtained (see Table 1).

This procedure can be scaled down to 1 A_{260} unit polynucleotide/0.1 ml, with a similar high efficiency of precipitation. We also scaled up the reactions to 50 mg DNA, obtaining 80 mg ± 15 mg DNA-chitosan precipitate, with a 2-5% loss of DNA into the supernatant.

Bisulfite-mediated deamination of cytosine in DNA Either native DNA (calf thymus), denatured DNA, native DNA-chitosan, or heat denatured DNA-chitosan (each 1 mg/ml PBS) was mixed with an equal volume of 2 M or 4 M sodium bisulfite (pH 5), and the mixture was allowed to stand at 37°C for 20 h. For the reaction of DNA-chitosans, the supernatant was discarded and the precipitate was washed with PBS and then treated with 1 M NH_4Cl-NH_3, pH 9.0, at 37°C for 5 h. For the reaction of DNA with bisulfite in solution, DNA was precipitated after the reaction with 3 vol. cold ethanol, dissolved in water, and subjected to dialysis against water. The dialyzed solution was lyophilized and the DNA obtained was treated with 1 M NH_4Cl-NH_3, pH 9.

For analyzing the deamination, the treated DNA-chitosan was washed with PBS and subjected to enzymatic digestion into nucleosides.

Nuclease digestion of polynucleotides in chitosan complexes DNA in the DNA chitosan complex (1 mg) or in solution (0.5 mg) was treated as follows.

To digest into nucleosides, the material was incubated in 400 μl 7.5 mM Tris-HCl, pH 7.4, containing 100 μg DNase I (Sigma), 1.5 μmol $MgCl_2$, and 0.004 μmol coformycin at 37°C for 2 h with shaking. Next, 10 μl 1 M Tris-HCl, pH 8.9, 25 μg snake venom phosphodiesterase I (Funakoshi, Tokyo) and 10 μg alkaline phosphatase (Sigma) were added, and the mixture was further incubated at 37°C for 2 h. The supernatant (or the solution for the free DNA-reaction) was mixed with 3 vol. ethanol and the mixture was allowed to stand at -20°C overnight. After centrifugation to remove the precipitated proteins, HPLC analysis of the nucleosides was carried out.

To estimate the DNA content in DNA-chitosan, the insoluble complex was digested into mononucleotides by the procedure described above except that no alkaline phosphatase was used, and the UV absorption of the digest was determined.

Adsorption of reagents to polynucleotide-chitosan A solution of reagent in PBS, 1 ml, was mixed with polynucleotide-chitosan (3 mg) and the mixture was swirled at 30 rpm at room temperature (22 ± 2°C) for 90 min. Adsorption was determined by measuring the absorbance of the solution. As a control, chitosan (1.5 mg), prepared by precipitation from a 0.05 N-HCl solution with added alkali, followed by washing with water and methanol, was used in this adsoption experiment. The experiments were performed in duplicate and the average values are presented in this paper: generally the duplicates showed good reproducibility.

Results and Discussion

Polynucleotide-chitosan complexes As Table 1 shows, the yields of chitosan complexes from DNA were almost quantitative and those from RNA and polyribonulceotides were 65-89%. The release of DNA from the DNA-chitosan complex into aqueous solution was measured. At pH 2-7, no release was detected; e.g., on treatment of the DNA-chitosan complex with phosphate-buffered saline at pH 7 and 37°C for 26 h, DNA released into the aqueous phase was less than 0.05%. At pH 13, the DNA was released from the complex: on treatment with 0.1 N NaOH at 80°C for 1 h, about 90% of the DNA in the DNA-chitosan became soluble. The alkali-elutable DNA content in the complex was determined to be around 10 A_{260}/mg, which corresponded to about 50% of the weight of the precipitate (Table 1). The content can also be determined by treatment of the complex with nucleases; this indicates that the DNA in the complex is accessible to enzyme proteins. Insoluble chitosan complexes were obtainable from RNA and other polynucleotides and the results in Table 1 show that all these complexes have similar high polynucleotide contents, about 50% in weight.

Table 1 Yields and nucleotide content of polynucleotide-chitosan complexes

Polynucleotide	Precipitation efficiency[a] (%) (A_{260}/mg)	Weight of precipitate (mg from 10 mg polynucleotide)	Nucleotide content in precipitate[b]
DNA (Calf thymus)	95	14	9.5
Denatured DNA (Calf thymus)	97	14	8.5
DNA (Salmon testes)	97	19	9.3, 9.6[c]
RNA (*E. coli*)	89	23	7.0, 8.5[c]
RNA (Yeast)	79	18	10.5
Transfer RNA (Yeast)	74	15	10.6
Poly I.Poly C	67	18	6.7
Poly A	72	13	16.5
Poly G	66	12	15.0
Poly U	65	13	9.4, 8.7[c]
poly C	75	15	10.0

a) Determined spectroscopically from the absorbance of the supernatant of the reaction mixture and the washings of the precipitate.

b) Determined, unless otherwise indicated, by treatment of duplicate samples with 0.1 N NaOH at 80°C for 1 h. The A_{260} value is normalized to that of the parent polynucleotide at pH 7. The A_{260} values per mg of parent polynucleotides used were: native calf thymus DNA 13; denatured calf thymus DNA 17; native salmon testes DNA 18; RNA 19; transfer RNA 19; poly I.poly C 15; poly A 31; poly G 24; poly U 20; poly C 16.

c) Determined by enzymatic digestion; for DNA with DNase I and snake venom phosphodiesterase, and for RNA and poly U with RNase A.

Bisulfite modification of DNA in the chitosan complex (more details are described in ref. 1.) We investigated whether the DNA complexed with chitosan, thereby becoming insoluble, can be chemically modified by bisulfite, a single-strand specific, cytosine deaminating agent[2]. The deamination of the cytosine in the DNA of the complex took place almost as efficiently as in solution. The single-strand specific nature of this chemical reaction was retained for the DNA complexed with chitosan. Thus, about 35% of the cytosine was converted to uracil on treatment of the denatured DNA-chitosan with 2 M sodium bisulfite at 37°C for 20 h, while 44% deamination occurred for denatured DNA in

solution. No deamination took place for native DNA-chitosan or for native DNA in solution.

Binding of compounds to polynucleotide-chitosan

These insoluble polynucleotide-chitosans are expected to be useful in directly measuring the affinity of compounds for polynucleotides. We examined ethidium bromide, heterocyclic amines, and several other compounds for their binding. Carcinogenic heterocyclic amines are known to be formed on cooking meat and fish[3]. More than 10 different compounds in this class have been identified and most of them have three fused aromatic rings. These compounds are strongly mutagenic to bacteria[4]. No extensive studies, however, have been performed regarding the non-covalent binding of these compounds to polynucleotides[5,6].

Table 2 Adsorption of ethidium bromide, heterocyclic amines, and other compounds to DNA- and RNA-chitosans

Compound	(μM)	Adsorption[a] (%)		
		DNA-chitosan	RNA-chitosan	Chitosan
Ethidium bromide	20	92.9	94.3	0
Glu-P-1	20	12.5	15.4	3.7
IQ	20	15.8	23.7	0.8
MeIQx	20	11.2	25.8	0.6
PhIP	40	13.0	17.0	3.9
Trp-P-2	20	86.7	85.9	7.6
4-Nitroquinoline 1-oxide	40	0	0.8	0.4

a) Native calf thymus DNA-chitosan containing 5 mmol nucleotide/3 mg, and yeast RNA-chitosan containing 4 mmol nucleotide/3 mg were used in 1 ml of reaction mixture in PBS containing individual compounds. For control chitosan 1.5 mg was used.

The adsorption of ethidium in PBS to DNA-chitosan was very rapid, almost instantaneous. For Trp-P-2 and Glu-P-1, we examined the time required for equilibration and found that a plateau of adsorption was reached following a 90-min swirling period. With this technique, adsorption of compounds to large excesses of DNA- and RNA-chitosans were investigated and the results are summarized in Table 2. Ethidium was adsorbed to DNA- and RNA-chitosans almost quantitatively but not to chitosan itself. All of the heterocyclic amines tested showed adsorption to DNA and RNA.

Although they were adsorbed to varying degrees, individual compounds had similar affinities for DNA and RNA. 4-Nitroquinoline 1-oxide, a carcinogen, did not bind to either DNA or RNA.

More extensive studies were performed on 4 representative heterocyclic amines; IQ, MeIQx, PhIP, and Trp-P-2. These compounds were found to bind to denatured DNA more strongly than to native DNA (the details are reported in reference 1). The results with homopolyribonucleotides suggest that binding occurs preferentially to purine nucleotides, particularly to guanine nucleotides. It is noteworthy that many heterocyclic amines including IQ, MeIQx, PhIP and Trp-P-2 are known to form adducts in DNA mainly with guanine[5].

We have established a method for preparing polynucleotide-chitosan complexes. Oligo- and polynucleotides having chain lengths larger than 15-20 can be generally precipitated by this procedure. Single-stranded or denatured polynucleotides may be recovered using this procedure. We have shown that the DNA in the chitosan complex is reactive towards enzymes and DNA-modifying and -binding agents.

References

[1] Hayatsu H., Kubo T., Tanaka Y. and Negishi K. *Chem. Pharm. Bull.*, 1997: 45: 1363.

[2] Hayatsu H. In: *Progress in Nucleic Acid Research and Molecular Biology Vol. 16*, Academic Press, New York, 1976: 75.

[3] Sugimura T. *Mutation Res.*, 1985: 150: 33.

[4] Negishi T., Nagao M., Hiramoto K. and Hayatsu H. In: *Mutagens in Food: Detection and Prevention*, CRC Press, Florida, 1991: Ch. 2.2.

[5] Negishi K., Nagao M., Hiramoto K. and Hayatsu H. In: *Mutagens in Food: Detection and Prevention*, CRC Press, Florida, 1991: Ch. 2.3.

[6] Pezzuto J.M., Lau P.P., Luh Y., Moore P.D., Wogan G.N. and Hecht, S.M. *Proc. Natl. Acad. Sci. USA*, 1980: 77: 1427.

RHEOLOGICAL CHARACTERISTIC OF DIBUTYRYLCHITIN SEMI-CONCENTRATED SOLUTIONS AND WET SPINNING OF DIBUTYRYLCHITIN FIBRES

Lidia SZOSLAND, Technical University of Łódź, Żeromskiego 116, 90-543 Łódź, (POLAND), fax +48 42 36 57 67, e-mail address: lidland@lodz1.p.lodz.pl;
Włodzimierz STĘPLEWSKI, The Institute of Chemical Fibres, Skłodowskiej-Curie 17/19, 90-570 Łódź (POLAND), fax + 48 42 37 62 14

Abstract

Rheological properties of semi-concentrated solutions (13%-20%) of dibutyrylchitin (DBCH) in dimethylformamide (DMF) were investigated and suitable conditions for wet spinning of DBCH fibres were found. The fibres properties were affected by molecular weight of polymer and spinning process conditions. A part of DBCH fibres was hydrolized with NaOH in water solution to produce converted chitin fibres with improved mechanical properties.

Keywords: dibutyrylchitin, rheological properties, shear viscosity, activation energy, wet spinning, fibre properties, chitin fibres.

Introduction

Dibutyrylchitin (DBCH) [1,2] is a bioactive [3] and biodegradable [4] chitin derivative, soluble in several popular organic solvents and able to form fibres. First attempt to create DBCH fibres was made using dry spinning of its solution in acetone [5-7]. It was found that DBCH fibres had tensile properties similar to or better than those of chitin and some chitin derivatives described in literature [5]. In this study the preparation of DBCH fibres using widespread method of spinning - a wet spinning procedure - is described and tensile properties of obtained fibres are presented. Results of rheological studies of DBCH solutions in dimethylformamide (DMF), carried out ahead of spinning procedure, are also presented.

Materials and methods

DBCH with degree of esterification equal to 2 was prepared using the method previously described [5]. Three samples of polymer with different molecular weights characterized by intrinsic viscosity values (determined in DMF at 25 °C) of 2.13, 1.92 and 1.53 dL/g were used in investigation of rheological properties of semi-concentrated solutions (13% - 20%, w/w) of DBCH in DMF. Measurements of shear viscosity values were made using a rotation rheometer with a concentric cylinder, Rheotest 2, Germany, in a range of shear rates γ from 0.1667 to 145.8 s^{-1}. The investigations were carried out at 25, 30 and 35 °C.

Wet spinning of DBCH fibres was made on apparatus commonly used for preparation of rayon fibres. A typical dope containing 15 - 19% of DBCH in DMF without filtration was added to the reservoir of the spinning system and extruded through a spinnret (300 holes, 80 μm diameter of the hole) to a coagulation bath. The filaments were coagulated in water, drawn in hot water, collected on rollers with a rate of 40 m/min and dried. A part of formed DBCH fibres was placed into 5% NaOH water solution and exposed to hydrolitic treatment with alkali in the time of 3-9 min at the temperature of 90 °C. Obtained chitin fibres were diligently washed and dried.

Results and discussion

DBCH solutions are stable in the organic solvents such as acetone, DMF, methanol, ethanol and some others. In DMF does not occur the process of DBCH degradation in finite time, an aggregation of macromolecules happens insignificantly in semi-concentrated solutions during the time of dope storage (light increase of the viscosity value η_0 at the shear rate $\gamma=0\ s^{-1}$), DMF is permissible as polymer solvent in the processes of fibre spinning on a technological scale - that is why it was chosen as a solvent of DBCH for the wet spinning procedure.

Rheological properties of DBCH solutions have been not investigated yet. The measurements were made in a range of shear rates from 0.1667 to 145.8 s^{-1} for DMF solutions of three samples of DBCH with different intrinsic viscosity values ($[\eta]_1=2.13$, $[\eta]_2=1.92$ and $[\eta]_3=1.53$ dL/g), with different concentrations of polymer (13, 15, 17, 19 or 20%, w/w) at temperatures of 25, 30 and 35 °C. In every case a linear dependence of shear stress τ [N/m^2] on shear rate γ [s^{-1}] was obtained in the equation $\tau = A\gamma^{n}$ (**A** and **n** are rheological parameters derived from the double log curve of shear stress-shear rate relationship). Determined values of **n** were located in the following ranges:

for the solutions of DBCH with $[\eta]_1=2.13$ dL/g $0.91 < \mathbf{n} < 0.96$
for the solutions of DBCH with $[\eta]_2=1.92$ dL/g $0.92 < \mathbf{n} < 0.98$
for the solutions of DBCH with $[\eta]_3=1.53$ dL/g $0.96 < \mathbf{n} = 1.00$

Value of **n** less than 1 increased with the decrease of the molecular weight of polymer and the concentration of solution and increased with the increase of the temperature. The solutions of DBCH with the intrinsic viscosity value $[\eta]_3=1.53$ dL/g and the concentrations the polymer of 15% and 17% behave at 30 and 35 °C as Newtonian shear thinning fluids with the **n**-parameter equal 1. The other investigated solutions of DBCH are very close to the Newtonian fluids (the **n**-parameter is very close to 1). The graphical relationship between lgη (η-shear viscosity values, $\eta=\tau/\gamma$, [Pa.s]) and lgτ (τ-shear stress values, [N/m^2, Pa]) typical for all investigated solutions of DBCH is presented in Figure 1. The non-linear dependence was observed for every system with a maximum value of the shear viscosity at $\tau=63.1\ N/m^2$. The primary increase of the shear viscosity values with the increase of the shear stress values is caused by prevailing unfluence of a longitudinal component on the vector of the shear viscosity at low shear rates [8].

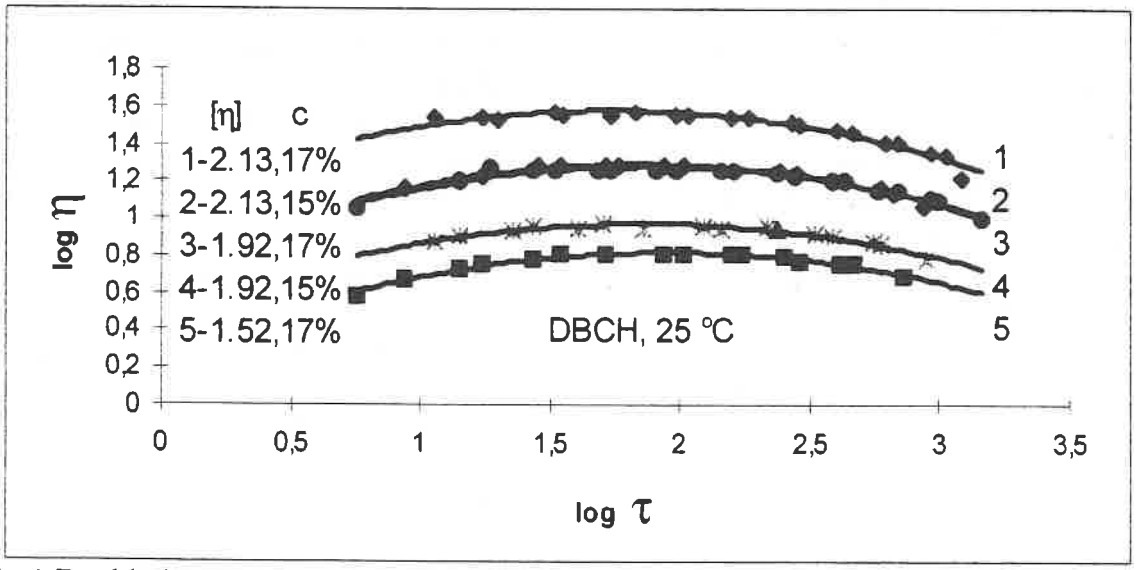

Fig.1.Double log curves: lg η versus lg τ (η-shear viscosity [Pa.s]; τ-shear stress [Pa])

A linear relationship of maximum shear viscosity values η_{max} at τ=63.1 N/m^2 from temperature of viscous solutions of DBCH in DMF is presented in Figure 2.

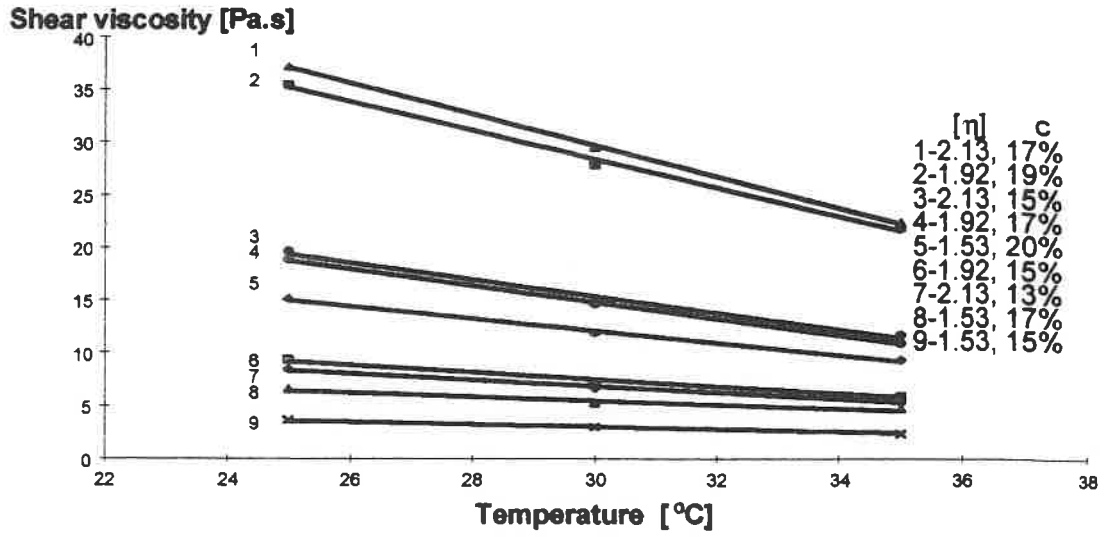

Fig.2. Relationship between the maximum shear viscosity values (at τ=63.1 N/m^2) and the temperature of DBCH solutions in DMF

The activation energy E_a of the viscous flow of the DBCH solutions at τ=63.1 N/m^2 was determined from the plot of $\ln(\eta_{max})$ - 1/T relationship of Arrhenius-type equation $1/\eta = A_0 \exp(-E_a/RT)$, where A_0 is a constant, K is the gas constant, T is the temperature [K]. The Arrhenius plots drawn for various concentrations and various molecular weights of the DBCH is shown in Figure 3, calculated values of E_a are collected in Table 1.

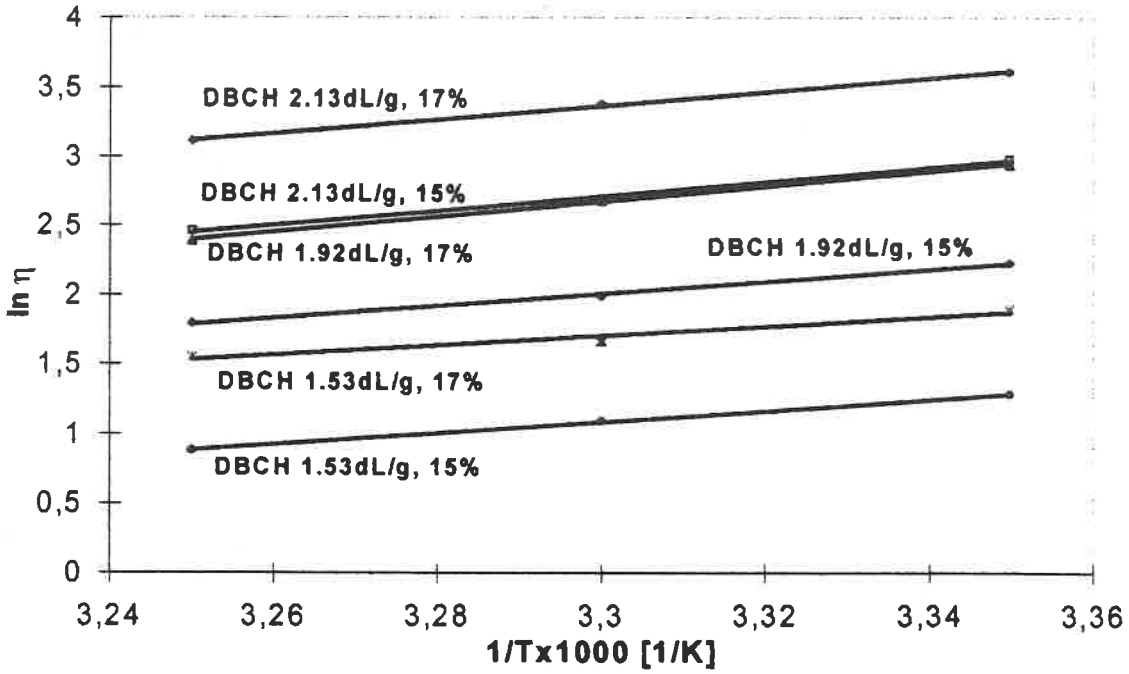

Fig.3. Arrhenius plot of DBCH solutions in DMF at τ = 63.1 N/m^2

As it was expected, the activation energy values increased with the increase of the molecular weight of the DBCH samples and with the increase of the concentrations of DBCH solutions.

Table 1

Activation energy of viscous flow of DBCH solutions in DMF at shear stress 63.1 N/m^2

Intrinsic viscosity of DBCH [η] [dL/g]	DBCH concentration [%]	E_a [KJ/mol]	Intrinsic viscosity of DBCH [η] [dL/g]	DBCH concentration [%]	E_a [KJ/mol]
2.13	17	44.1	2.13	15	41.6
1.92	17	43.2	1.92	15	36.6
1.53	17	28.5	1.53	15	26.8

The determined values of shear viscosity η_{max} at shear stress τ =63,1 N/m^2 for all studied solutions of DBCH in DMF are collected in Table 2. It was found that the molecular weight has a prevailing influence on the viscosity of DBCH solutions: descrease the intrinsic viscosity value from $[\eta]_1$=2,13 to $[\eta]_3$=1.53 dL/g caused the most significant descrease in the shear viscosity (ca 80%). The increase of the temperature from 25 to 35 °C and decrease of the solution concentration from 17% to 15% of DBCH caused the decrease in the shear viscosity for 35 - 47% depended on the molecular weight of DBCH's.

Table 2

Shear viscosity values η_{max} determined for DBCH solutions in DMF at τ = 63.1 N/m^2

Intrinsic viscosity of DBCH, [η] [dL/g]	DBCH concentation in DMF [%]	Temperature of solution [°C]	Shear viscosity η_{max} at τ = 63.1 Pa [Pa.s}
2.13	17	25	37.15
		30	29.51
		35	22.39
2.13	15	25	19.72
		30	14.79
		35	11.75
2.13	13	25	8.41
		30	6.68
		35	5.37
1.92	19	25	35.48
		30	27.86
		35	21.88
1.92	17	25	18.84
		30	14.62
		35	10.96
1.92	15	25	9.33
		30	7.77
		35	5.96
1.53	20	25	15.14
		30	11.91
		35	9.33
1.53	17	25	6.61
		30	5.25
		35	4.69
1.53	15	25	3.63
		30	2.99
		35	2.40

The choise of DBCH concentratios to be used for first spinning trials was decided upon results of the rheological investigations.The near Newtonian or exact Newtonian behavoir and comparatively low the shear viscosity values of the DBCH in DMF solutions permitted to use 15 -19% DBCH solutions as a dope.

The spinning solutions were prepared by dissolving the proper amount of polymer at room temperature. DBCH dissolved in DMF completely, and the spinning solution was introduced without filtering into a dope reservoir of a laboratory scale spinning apparatus, commonly used for the wet spinning of rayon fibres. Fibres spinning was carried out without difficulty, coagulation of polymer proceeded in water, formed wet fibres were strong enough to be fourfold drown in hot water. The fibres were wound up at the rate of 40 m/min on rollers and dried in air.The obtained fibres had a round cross-sections, smooth surfaces, the individual filaments were well separated. The influence of spinning procedure parameters on the mechanical properties of formed fibres was investigated and optimum conditions of the wet spinning were found. A method of preparation of new DBCH fibres is being patented, therefore details of the process can not be described.

A kinetic of an alkali hydrolysis reaction of the DBCH, provided under heterogeneous conditions, was studied previously and results were published [9]. It was found that controlled hydrolysis of DBCH fibres created by dry spinning of its solution in acetone, carried out in water solutions of NaOH, produced chitin fibres without destroying their structure with better tensile properties than initial DBCH fibres [5]. The similar procedure was applied to produce the chitin fibres from the DBCH fibres spinned by the wet method.

A part of the DBCH fibres, created by the wet spinning from the sample with $[\eta]_i$= 2.13 dL/g, were dipped into 5% NaOH water solution and heterogeneously hydrolized at 90 °C in time of 3 or 9 minutes. After washing the hydrolized fibres in water several times, then in dilute solution of acetic acid and then in water again, the chitin fibres, insoluble in the organic solvents, were obtained. The chitin fibres were dried in warm air at 50 °C. Tensile properties of the DBCH and chitin fibres were investigated; typical results obtained are collected in Table 3 and compared with the previously reported tensile properties of chitin fibres, prepared from DBCH fibres formed by the dry spinning method [5].

Table 3

Yarn properties of DBCH and chitin fibres

No	Sample	Method of fibre preparation	Yarn count [tex]	Tenacity [N/tex]	Elongation [%]
1	DBCH, [η]=1.53 dL/g	wet spinning	35,5	0.165	7.4
2	DBCH, [η]=1.92 dL/g	wet spinning	23.3	0.192	5.9
3	DBCH, [η]=2.13 dL/g	wet spinning	48.7	0.161	7.1
4	Chitin from sample No3	Hydrolysis in 5% NaOH, 90°C, 3 min	39.5	0.220	8.9
5	Chitin from sample No3	Hydrolysis as above, in time of 9 min	13.3	0.266	9.8
6	Chitin [5]	Hydrolysis of DBCH fibres prepared by dry spinning [5]	42.4	0.250	35.4

The results presented in Table 3 showed the good tensile properties of the DBCH fibres prepared on the common apparatus used for the wet spinning of the rayon fibres. Alkali hydrolysis of the polymer leads again to converting of the DBCH fibres to the chitin fibres with improved tensile properties. The good mechanical properties of the DBCH and chitin fibres create a possibility to form a wide assortiment of chitin and chitin derivative materials for biomedical applications.

Conclusion

1. For the first time the rheological properties of the dibutyrylchitin semi-concentrated solutions were investigated and suitable concentrations of the polymer were chosen for the first wet spinning trials.
2. New dibutyrylchitin fibres were created by the wet spinning of its 15-19% solutions in dimethylformamide on the common apparatus used for spinning of the rayon fibres.
3. The spinning process proceeded without difficulties. The fibre properties were affected by the molecular weight of the polymer and the spinning condition. Fibre tenacities up to 0.20 N/tex were obtained.
4. The dibutyrylchitin fibres can be converted into chitin fibres with improved tensile properties by treatment of them with water solutions of NaOH.
5. The good mechanical properties of the DBCH and chitin fibres create a possibility to form a wide assortiment of chitin and chitin derivative materials for biomedical applications.

References

1.K.Kaifu, N.Nishi, O.Somorin, J.Noguchi: Studies on chitin. V.Formylation, propionylation and butyrylation of chitin. ***Polym.J. 13,*** *241 (1981).*

2. L.Szosland: Synthesis of highly substituted butyrylchitin in the presence of perchloric acid. ***J.Bioactive and Compat.Pol. 11,*** *61 (1996)*

3. J.Dutkiewicz, L.Szosland, M.Kucharska, L.Judkiewicz, R.Ciszewski: The effect of solid chitin derivatives on blood coagulation. ***J.Bioactive and Compat.Pol. 5,*** *293 (1990).*

4. L.Szosland, J.Szumilewicz, H.Struszczyk: Enzymatic degradation of dibutyrylchitin, ***Chitin Enzymology, vol 2,*** *Proceedings of the 2nd International Symposium on Chitin Enzymology, ed. by R.A.A.Muzzarelli, 1996, 491, Senigallia, Italy,*

5.L.Szosland, G.E.East: The dry spinning of dibutyrylchitin fibers. ***J.Appl.Pol.Sci. 58,*** *2459 (1995).*

6. L.Szosland: Preparation of butyrylchitin fibers. ***Chitin World,*** *Proceedings from the 6th International Conference on Chitin and Chitosan, 1994, 209, Gdynia, Poland*

7. L.Szosland: A simple method for the production of chitin materials from the chitin ester derivatives. ***Advances in Chitin Science, vol.1,*** *Proceedings of the 1st Internatinal Conference of the European Chitin Society, 1995, 297, Brest, France.*

8.A.Ziabicki: „Fizyka procesów formowania włókien", *WNT Warszawa, 24-34, 1970.*

9.L.Szosland: Alkaline hydrolysis of dibutyrylchitin:Kinetic and selected properties of hydrolysis products. ***Fibres & Textiles in Eastern Europe 4,*** *76 (1996).*

Acknoledgements

This work is supported by the Committee for Research, Poland, in the framework of the project nr 3 TO9 B 021 08.

MORPHOLOGY AND PHYSICAL PROPERTIES OF BIODEGRADABLE CHITOSAN BLENDS CONTAINING PVA AND PEO

Joanna PIEKIELNA, Maria MUCHA, Marcin SZWARC,
Faculty of Process and Environmental Engineering, Technical University of Łódź, ul. Wólczańska 175, 90-924 Łódź, (Poland). Fax: 0 48 42 36 49 23
E. Mail: muchama@wipos.p.lodz.pl

Abstract

Biodegradable chitosan films of about 30 μm thick containing poly(ethylene oxide) and poly(vinyl alcohol) were prepared by mixing PEO or PVA aqueous solutions with a chitosan acetate solution in appropriate amount and their films were prepared by casting method.

Both blends are found to be homogeneous. In the blends with crystallizable component the chitosan locates in interlamellar regions of PEO spherulites and does not form any visible domains. The melting temperature and the degree of crystallinity of PEO decrease with increasing chitosan content. Flory-Huggins interaction parameter was equal -0.36 and indicates good miscibility of chitosan with PEO. Kinetics of crystallization process of PEO in the films was investigated by DSC and described by Avrami equation. Single Tg of PVA/chitosan blends is observed. The presence of chitosan rises the value of initial temperature of thermal degradation of POE and PVA in the films with chitosan.

Keywords: chitosan, poly(ethylene oxide), poly(vinyl alcohol), morphology, physical properties, DSC, kinetics of crystallization

Introduction

Polymer blends containing biodegradable components have received much interest because of the ease with which their physical properties and ability to degradation can be modified. These materials have attracted much attention especially in relation to applications in disposables and biomedical uses. Some blends of this type have been described, for instance mixtures of poly(ethylene oxide) (PEO) and poly(vinyl alcohol) (PVA) with chitosan acetate salt or poly(L-lactide) (PLLA) [1-3]. In this paper we present the morphology and thermal behaviour of PEO, PVA blends with chitosan.

Materials and methods

Three polymer materials were studied: poly(ethylene oxide) (PEO) of molecular weight $M_w = 10^4$ obtained from Polysciences Inc., poly(vinyl alcohol) (PVA), a commercial product of low M_w, and chitosan. PEO is a polymer of a high degree of crystallinity, in contrast to PVA which is characterised by low crystallinity. A characteristic feature of the two substances is solubility in water which is very suitable when preparing homogeneous mixtures [4-7]. The chitosan used in the investigations was produced in the Sea Fishery's Institute (Gdynia) and had molecular weight $M_w = 4.5*10^5$; its deacetylation degree was DD = 73.3%.

Morphology and some physical properties of synthetic polymer (PEO and PVA) blends with chitosan were investigated in the study. Films made of these blends were obtained from a polymer solution of a relevant weight ratio of components ranging from 10 to 90% weight fraction of chitosan. The films produced were homogeneous and transparent (until 30% weight fraction of PEO), which shows homogeneity of the mixture of particular components [8].

Investigations of the morphological structure of the samples were carried out using a polarizing microscope. The image of the sample being analysed was observed directly in the microscope or by a video camera installed on the microscope, using the MultiScan computer analysis program.

To determine the melting point (T_m), temperature of thermal degradation onset (T_d), energy effects such as enthalpy (ΔH_f) and entropy of melting (ΔS_f) or heat of degradation (ΔH_d), and to describe process kinetics of crystallization of the blends the differential scanning calorimetry (DSC) was used. Measurements were made using the Mettler FP 85 device for temperatures ranging from 20 to 100°C at a standard heating rate of 10°C/min. When investigating thermal degradation of blends in air condition, a series of measurements were carried out at elevated temperature up to 220°C. Because of the presence of water residues in the samples, the DSC investigations were carried out additionally at re-heating.

Figure 1 shows thermograms of first and second runs of the DSC analysis of selected PEO/chitosan systems. Curves representing subsequent runs for the same sample differ by the presence of a broad peak of heat of water evaporation at temperature 100°C. The presence of water affects also the decrease of the melting point of PEO. On the basis of first DSC runs of PEO/chitosan samples being analysed, relationships of the residue water amount in the systems containing this solvent were drawn (Fig. 2). In the case of PVA/chitosan systems, the peak of heat of water evaporation observed in the first run disappeared in the second run.

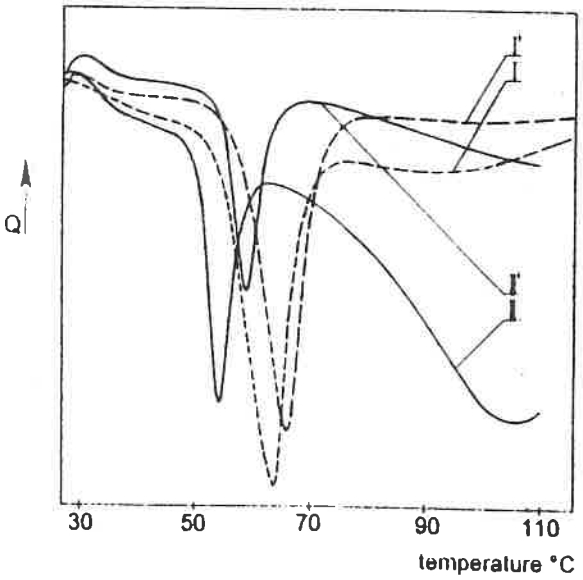

Fig. 1. DSC thermograms of first ( ) and second (') runs of PEO/chitosan systems in weight ratios: I.) 0.7:0.3; II.) 0.2:0.8

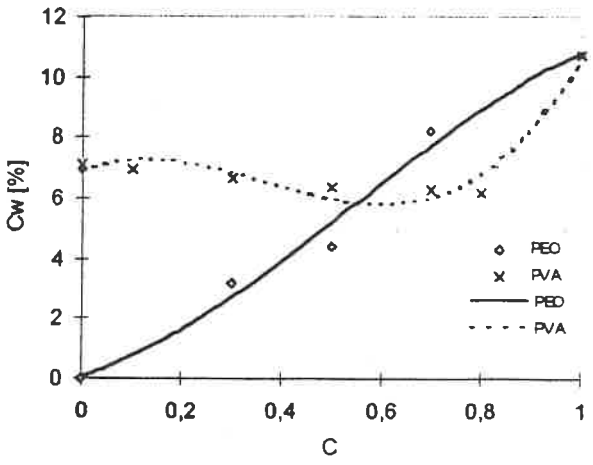

Fig. 2. Water content in PEO/chitosan, PVA/chitosan systems according to weight fraction of chitosan

To investigate crystallization kinetics of the blends, a four-stage run of the DSC measurement was established. At the first stage, the sample was heated to temperature

90°C at the rate 10°C/min. and was kept at that temperature for 2 minutes. Next, the sample was cooled rapidly to the temperature of isothermal crystallization. The differential curves were transformed into integral curves which were described by the Avrami equation [9]. The analysis of crystallization kinetics enabled to determine coefficients in the Avrami equation describing the type of nucleation and crystallization in the process of crystalline structure formation in the PEO/chitosan blend.

Results and discussion

Morphology of the samples

Microphotographs of morphological structure of PEO blends with chitosan made by means of polarizing microscope and computer image analyzer are shown in Fig. 3. They reveal a dependence of the structure and size of PEO spherulites on biopolymer fraction. Chitosan macromolecules are closed in the interlamellar amorphous regions of growing spherulites thus causing their modification. The fraction of chitosan in the mixture limits the PEO nucleation process which leads to formation of larger spherulites [2]. A clear spherulitic structure is formed up to 0.5 weight fraction of chitosan in the sample. At an increasing chitosan content, the crystallization of PEO becomes difficult until an amorphous structure of the homogeneous blend is obtained.

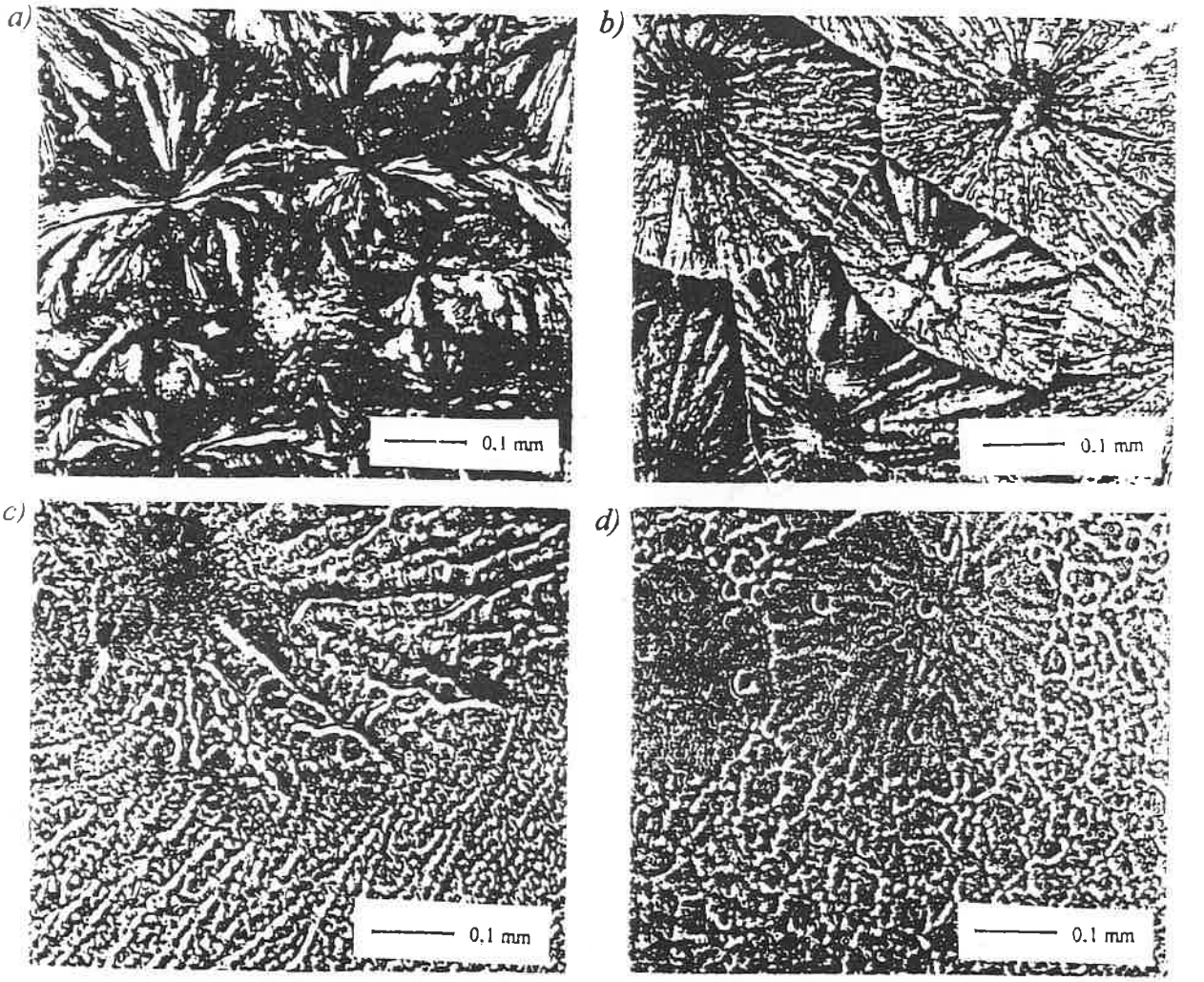

Fig. 3. Polarizing microscope microphotographs of: a) pure PEO; and blends of PEO/chitosan at ratio: b) 0.8:0.2; c) 0.5:0.5; d) 0.2:0.8.

DSC analysis

DSC investigations showed the presence of residual water in the analyzed samples which clearly decreased the melting point of PEO and chitosan in the whole range of miscibility. Figure 4 illustrates these differences between the first and second DSC runs. The differences ranged from 2 to 6 K, depending on the weight fraction of chitosan, and so – also on the percent of water in the sample. For further analysis of the samples only second DSC runs were used (Fig. 5).

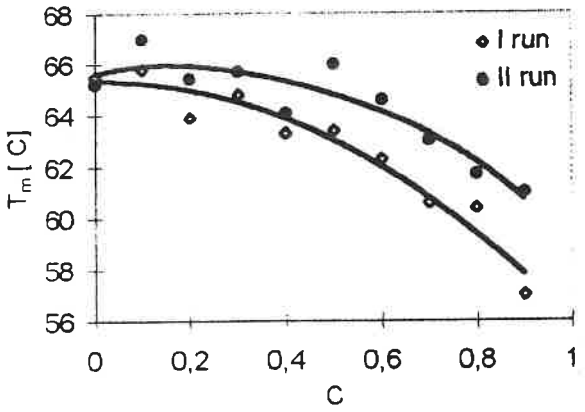

Fig. 4. Melting point of PEO/chitosan blends as a function of weight fraction of chitosan from two subsequent DSC runs

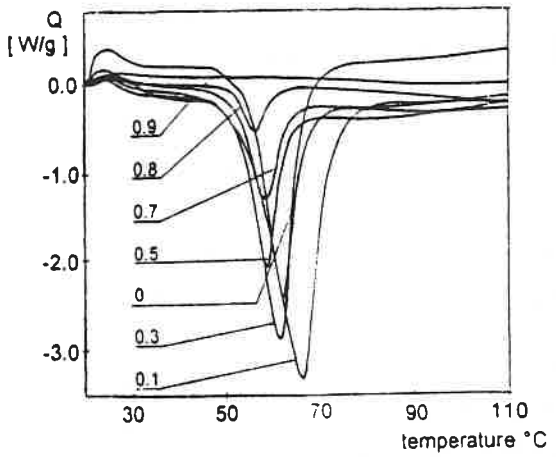

Fig. 5 Second DSC runs for PEO/chitosan systems and a description of weight fractions of chitosan

On the basis of melting points determined and using eq. (1) the degree of crystallinity of PEO in the blend was determined:

$$X=\Delta H_0/\Delta H_{100\%PEO} \quad (1)$$

ΔH_0 – heat of melting of polyethylene oxide in chitosan blend (converted into PEO weight fraction); $\Delta H_{100\%PEO}$ – heat of melting of crystalline 100% PEO equal 222.07 J/g.

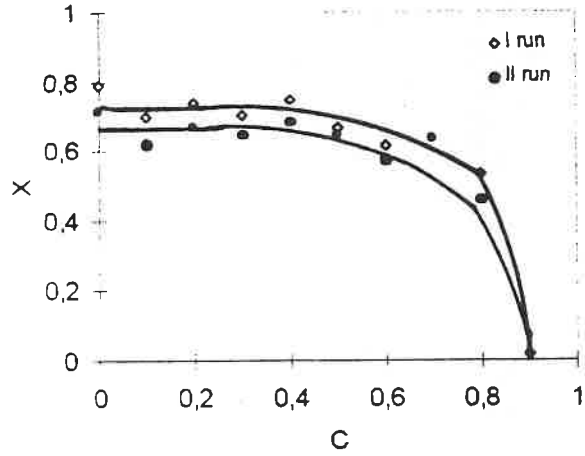

Fig. 6. Dependence of crystallinity degree of PEO/chitosan system on the weight fraction of chitosan

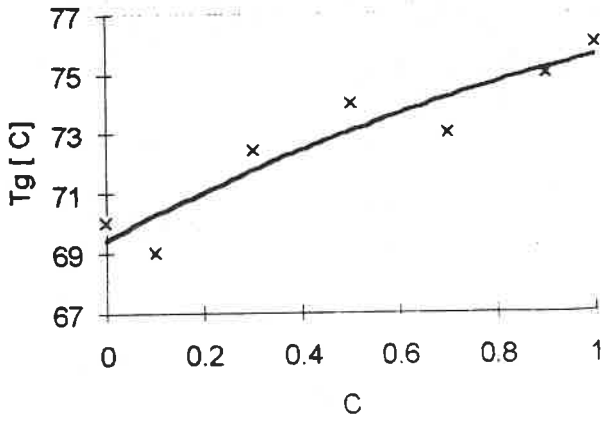

Fig. 7. Glass transition temperature of PVA/chitosan systems as a function of the weight fraction of chitosan

The degree of crystallinity of pure PEO was 0.79 and this value remains approximately constant up to 0.4 weight fraction of chitosan in the blend, and next it decreases with increasing weight fraction of chitosan in the sample, which is shown in Fig. 6. DSC studies confirm the conclusions drawn from a microscopic observation of

sample morphology: the lower PEO content in the blend with an amorphous polymer, the lower is the crystallinity degree of PEO as part of the polymer molecules did not crystallize [10].

The temperature of PVA glass transition was read out from second runs of DSC (after water removal) and was equal 70°C. The mixtures had a single glass transition temperature whose value increased with the weight fraction of chitosan, a feature which confirms good miscibility of components in the blend (Fig. 7).

Figure 8 shows Avrami relationship for PEO/chitosan blends at temperature 48°C from Avrami equation (2). After longer crystallization process (above 7 min.) a secondary crystallization of PEO chains is observed. Average value of Avrami exponent is n = 2.2.

$$\log(-\ln(1-v^c)) = \log K + n \log(t) \qquad (2)$$

K – rate constant, n – Avrami exponent, v^c – relative crystallinity, $v^c = X(t)/X(\infty)$, $X(t)$, $X(\infty)$ – absolute and equilibrium crystallinity degree, t – time.

Specific interactions between components can be described by the Flory-Huggins thermodynamic interaction parameter χ_{12} which characterizes the dimensionless interaction free energy mixing and is typically used as a measure of the enthalpic and entropic excess contributions to potentially favourable mixing. The interaction parameter is accessible from the following simplified equation [12,13,14]:

$$\frac{1}{T_{mb}} - \frac{1}{T_{mp}} = -\left(\frac{RV_{2u}}{\Delta H_{2u} V_{1u}}\right)\chi_{12} V_1^2 \qquad (3)$$

T_{mb}, T_{mp} – melting temperatures (in blends and pure polymer) were taken instead of equilibrium melting temperature T_{mb}^0 and T_{mp}^0; V_1 – the volume fraction of chitosan, V_{1u} – the repeat unit molar volume of chitosan, 132.5 cm^3/mol; V_{2u} – the repeat unit molar volume of PEO, 39.3 cm^3/mol; ΔH_{2u} – the enthalpy of fusion for completely crystalline PEO, 222.07 J/g.

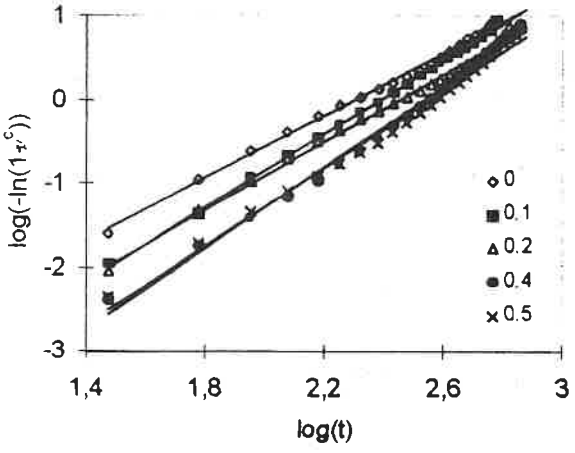

Fig. 8. Avrami relationship for PEO/chitosan blends at temperature 48°C in reference to weight fraction of chitosan in the mixture

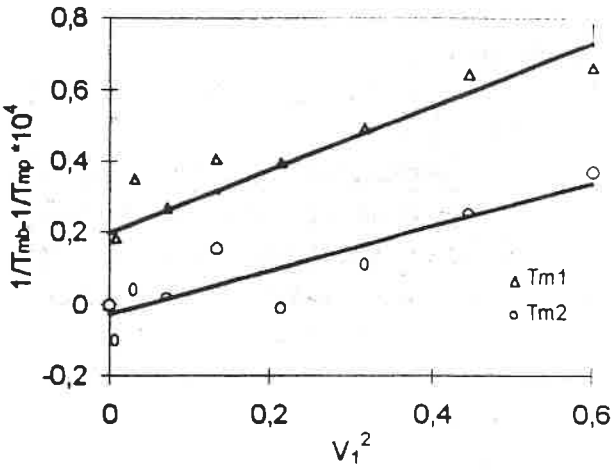

Fig. 9. Graphical presentation of equation (3) for determination of the interaction coefficient (for melting temperatures from the first (T_{m1}) and second (T_{m2}) DSC run).

On the basis of eq. (3) and Fig. 9 the interaction coefficients (χ_{12}) were determined. For blends obtained from the solution (T_{m1}) – first run, this coefficient is

χ_{12} = -0.36, while after melting (T_{m2}) – second run χ_{12} = -0.24. This negative value of χ_{12} is consistent with miscible system and clearly indicates that the miscibility of PEO and chitosan is driven by strong specific interactions in the amorphous phase. The absolute value of the interaction coefficient changes with morphological state of the sample and perhaps a presence of residual water.

Conclusions

Microscopic studies of morphological structure of PEO/chitosan blends reveal a dependence of the structure and size of PEO spherulites PEO on chitosan fraction. During crystallization, macromolecules of chitosan are closed in interlamellar amorphous regions of growing spherulites thus causing their modification. Chitosan fraction in the blend reduces PEO nucleation which leads to formation of bigger spherulites . The DSC analysis showed the presence of residual water in both types of PVA/chitosan and PEO/chitosan blends. The PVA/chitosan blends had a single glass transition temperature which increased with weight fraction of chitosan. This points to good miscibility of components in the blend.

The degree of crystallinity remains approximately constant up to 0.4 weight fraction of chitosan in the blend. The analysis of integral curves of isothermal crystallization process and coefficients determined for Avrami equation show that the PEO crystallization slowed down with an increase of weight fraction of chitosan in the blend ($n \approx 2$, K - decreasis).

The absolute value of the interaction coefficient determined on the basis of temperature decrease T_m for PEO in the blend (diluent effect), changes with thermal history of PEO/chitosan systems. For mixtures obtained directly from the solution (T_{m1} in the first run) this coefficient is χ_{12} = -0.36, while after crystallization from melt (T_{m2} in the second run) χ_{12} = -0.24. This negative value of χ_{12} is consistent with miscible system and clearly indicates that the miscibility of PEO and chitosan is driven by strong specific interactions in the amorphous phase.

References

1. A. J. Nijenhuis, E. Colstee, D. W. Grijpma, A. J. Pennings, Polymer, 1996, 37, 26, 5849-5857
2. A. Wrzyszczyński, Xia Qu, L. Szosland, E. Adamczak, L. A. Linden, J. F. Rabek Polymer Bulletin, 1995, 34, 493-500;
3. Ch. Nakafuku, Polymer Journal, 1996, 28, 7, 568-575;
4. K. Petrenko, V. Privalko, Yu. Lipatov, Polymer, 1990, 31, 1283-1287;
5. Z. Bartczak, E. Martuscelli, Makromol. Chem., 1987, 188, 445-453;
6. S. Cimino, E. Di Pace, E. Martuscelli, C. Silvestre, Makromol. Chem., 1990, 191, 2447-2454;
7. J. Rault, Z. Ping, Q. Nquyen, Polymer Bulletin, 1995, 35, 649-652;
8. M. Miya, R. Iwamoto, S. Mima, Journal of Polymer Sience, 1984, 22, 1149-1151;
9. M. Avrami, J. Chem. Phys. , 1940, 8, 212;
10. M. Mucha, Colloid Polym. Sci., 1994, 272, 1090-1097;
11. N. Angelova VI Międzynarodowa Konferencja „Chitin and chitosan", Gdynia 1993.
12. T. Nishi, T. Wang, Macromolecules, 1975, 8, 909;
13. Ch. Qin, A. Pires, L. Belfiore, Polymer Com., 1990, 31, 177-182;
14. J. Sotele, V. Soldi, A. Pires, Polymer, 1997, 38, 5, 1179-1185

CHITOSAN-CALCIUM ALGINATE HYDROGELS AS A NOVEL INTERMEDIATE FOR CALCIFICATION OF AQUEOUS HYDROGEN CARBONATE IONS BY MIMICKING CRAB'S SHELL FORMATION

Shigehiro HIRANO,[1,2] Koichi YAMAMOTO,[2] Hiroshi INUI,[2] Kurt I. DRAGET,[3] Kjell M. VARUM,[3] and Olav SMIDSROD[3]

[1]Chitin/Chitosan R&D Institute, 445-Sakuradani, Tottori 680 (Japan), [2]Department of Agricultural Biochemistry and Biotechnology, Tottori 680 (Japan), and [3]Department of Biotechnology, University of Trondheim, N-7034, Trondheim (Norway)

Abstract

The present work aims to develop a novel method for the fixation of aqueous HCO_3^- ions as $CaCO_3$ by mimicking the biomineralization of crab shells. A novel transparent hydrogel of chitosan-calcium alginate composite was prepared and used as an intermediate for holding calcium ions in water. The hydrogel was soaked in 0.1 M aq. $NaHCO_3$ solution (pH ca. 8) at room temperature for 1 day to afford a chitosan-$CaCO_3$ composite as a precipitate (61% chitosan and 22% CO_3^{2-}):

Chitosan-Ca alginate + $NaHCO_3$

$\rightarrow$ Chitosan-$CaCO_3$ + Na alginate + CO_2 + H_2O

The Na alginate was recovered from the filtrate as a precipitate by addition of 3 volumes of EtOH.

Keywords: alginate, chitosan, chitosan-$CaCO_3$ composite, CO_3--fixation, hydrogels.

Chitin and chitosan are homopolysaccharides and are found widely in many marine animal shells. Alginate is a heteropolysaccharide of (1→4)-linked β-D-mannuronic acid and α-L-guluronic acid residues, and is found in various seaweeds. Calcium carbonate is the main structural component of crab shells, seashells and coral reefs. Crab shell consists of $CaCO_3$, chitin and protein as the main components [1]. In crab shell ecdysis, $CaCO_3$ in the shell is solubilized into the body fluids and into the specific organs. The solublilized Ca^{2+} ions are again utilized for the fixation of aq. CO_3^{+} ions in water into new shells [2-4]. Crabs assemble chitin fibrils into a cylindrical architecture at the endocuticle layer of shells, using the Ca^{2+} ions in the body fluids and aq. HCO_3^- ions in the hydrosphere [5,6]. The fixation of aq. HCO_3^- ions into coral reefs has been reported [7]. Sea water is slightly alkaline (pH 7.5-8.5) due to presence of several metal cations including Na^+, Mg^{2+} and K^+ [8].

In our previous works, several metal halides including $CaCl_2$, $CuCl_2$ and $ZnCl_2$ were used as a source of metal cations, and aq. Na_2CO_3 and $NaHCO_3$ solutions were used as a source of CO_3^{2-} ions [9,10]. As the result, aq. CO_3^{2-} ions were mineralized as chitin-$CaCO_3$, chitosan-$CaCO_3$, chitosan-$ZnCO_3$, and chitosan-$CuCO_3$. In these reactions, the large

part of $CaCl_2$ was released out of the gelatinous matrixes of chitin and chitosan during the treatment [6], and the maximum 0.44 mole CO_3^{2-} ions per GlcN (10% of total weight) was fixed as metal carbonates. It is essential to develop a new closed system for the mineralization of HCO_3^- ions in water. Zhang and Gonsalves [11] reported a crystal growth of $CaCO_3$ on chitosan molecule in a supersaturated $CaCO_3$ solution, but its detail is unknown. Taking these previous works into consideration, it is essential to develop an efficient and mild method for the mineralization of aq. HCO_3^- ions in the hydrosphere.

In the present work, we report a novel biomimic procedure for the fixation of aq. HCO_3^- ions into Ca alginate hydrogel and into chitosan-Ca alginate hydrogel by soaking in 0.1 M aq. $NaHCO_3$ solution (pH ca. 8) at room temperature.

Materials and Methods

A commercial sample (Flonac N, Kyowa Technos, Co., Ltd. Chiba, Japan) of crab shell chitosan was treated one time with 40% aq. NaOH at 100 °C for 4 h to give a purified sample of chitosan, MW 3 x 10^5; d.s. 0.1 for NAc; $[\alpha]_D^{20}$ -6° (*c* 0.8%, 2% aq. AcOH); ν_{max}^{KBr} 1620 cm^{-1} (NH_2) and no absorptions at 1650 and 1550 cm^{-1} (NAc). Sodium alginate (MW 36x10^5, 69% L-guluronic acid content) was a product (Protanal LF10160 SLP 466 isolated from a brown algae, *Laminaria hyperborea*) of Protan Co., Ltd., Norway. Alginate was analyzed by the carbazole reaction [12].

Calcium alginate hydrogel

A solution of Na alginate (0.50 g) in water (20 ml) was put into a dialysis membrane tube (diameter 1.5 cm), and soaked in 0.1M aq. $CaCl_2$ (500 ml) at room temperature overnight to afford a gel. The gel was dialyzed against running water and distilled water to give a transparent Ca alginate hydrogel.

$CaCO_3$ produced from a Ca alginate hydrogel by soaking in 0.1 M aq. $NaHCO_3$ solution

The above hydrogel obtained was put into a dialysis membrane tube, and was soaked in 500 ml of 0.1 M aq. $NaHCO_3$ solution (pH 8) with gentle stirring at room temperature for 1 day. Calcium carbonate appeared as a white precipitate, and Na alginate was solubilized. The precipitate was collected and dried to afford $CaCO_3$ (0.10-0.15 g), ν_{max}^{KBr} 1450, 870 and 710 cm^{-1} (CO_3^{2-}).

Chitosan-Ca alginate hydrogel

A solution of chitosan (0.30 g) in 0.2% aq. acetic acid (6 ml) was diluted with water (17 ml, pH about 6.5). To the solution was added a Na alginate (0.40 g) solution in 20 ml water, and a viscous transparent solution was obtained. The

solution was put into a dialysis membrane tube (diameter 1.5 cm) and soaked in 0.1 M aq. $CaCl_2$ solution (500 ml) overnight to afford a hydrogel in the tube. The hydrogel was dialyzed against distilled water overnight, and a transparent chitosan-Ca alginate hydrogel was obtained. The hydrogel was stable in boiling water, but unstable in aq. strong acid and alkaline solutions. Part of the hydrogel was lyophilized. Anal. N 3.72% (43% chitosan).

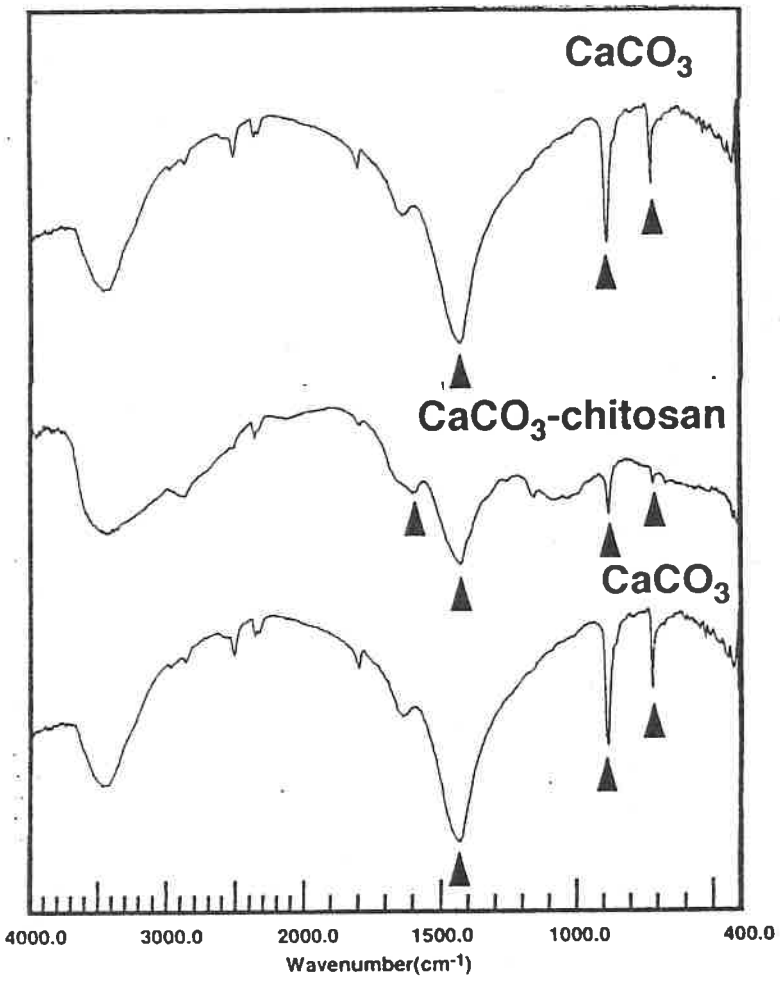

Fig. 1. FTIR spectra of $CaCO_3$ (top) and chitosan-$CaCO_3$ composite (middle), which were prepared from each of Ca alginate hydrogel and chitosan-Ca alginate hydrogel, and of an authentic $CaCO_3$ (bottom).

A chitosan-$CaCO_3$ composite formed from a chitosan-Ca alginate hydrogel by soaking in 0.1 M aq. $NaHCO_3$ solution

The chitosan-Ca alginate hydrogel obtained above was put into a dialysis membrane tube, and was soaked in 500 ml of 0.1 M aq. $NaHCO_3$ solution (pH about 8) at room temperature for 1 day. A chitosan-$CaCO_3$ composite appeared as a precipitate and Na alginate is solubilized. The precipitate was collected, soaked in distilled water for 1 day, and dried to afford a

white chitosan-$CaCO_3$ composite (0.40 g). ν_{max}^{KBr} 1425, 876 and 712 cm^{-1}(CO_3^{2-}). Anal. N 5.30% (61% chitosan). The composite was negative for the carbazole reaction, and contained 22% CO_3^{2-} as estimated from C/N ratio of the elemental analyses. The filtrate was concentrated *in vacuo* and the addition of 3 volumes of ethanol gave rise to Na alginate.

Results and Discussion

By soaking in 0.1 M aq. $NaHCO_3$ at room temperature, $CaCO_3$ was produced from the Ca alginate hydrogel, and a chitosan-$CaCO_3$ composite was produced from the chitosan-Ca alginate hydrogel as a precipitate. In the both cases, water-soluble Na alginate was produced. The presence of CO_3^{2-} ions was confirmed by their characteristic FTIR absorptions at 1450, 870 and 710 cm^{-1} (Fig. 1). The chitosan-Ca alginate hydrogel was colorless, transparent, stable in aq, alkaline solutions, unstable in aq. acidic solutions, and irreversible on heating and cooling.

The fixation mechanism of aq. HCO_3^- ions as $CaCO_3$ from the Ca alginate hydrogel is shown as the following equations:

Na alginate + $CaCl_2$ → Ca alginate + NaCl

Ca alginate + $2NaHCO_3$ →

$CaCO_3$ + Na_2 alginate + CO_2 + H_2O

The reaction mechanism for the fixation of aq. HCO_3^- ions as chitosan-CaCO3 from the chitosan-Ca alginate hydrogel is shown as the following equations:

Chitosan-Na alginate + $CaCl_2$ →

Chitosan-Ca alginate + 2NaCl

Chitosan-Ca alginate + $2NaHCO_3$ →

Chitosan-$CaCO_3$ + Na_2 alginate + CO_2 + H_2O

In the present fixation reactions of aq. HCO_3^- ions, one mole of aq. CO_3^{2-} ions was mineralized and one mole of CO_2 is liberated into water. The produced chitosan-$CaCO_3$ composite is usable as a functional feed additive for animals and fishes and for novel biotechnological materials [13]. The recovered alginate is usable repeatedly in the present experiment.

References

[1] Parsons T K, Takahashi M and Hargrave B. *Biological Oceanographic Processes*, 3rd Ed, 1984; 1: 55.

[2] Yano I. *Nippon Suisan Gakkaishi* 1972; 38:733.

[3] Yano I. *Nippon Suisan Gakkaishi* 1974; 40:783.

[4] Yano I. *Kagaku to Seibutsu* 1977; 15:328.

[5] Hirano S, Inui H, Yamamoto K. *Energy Convers Mgmt* 1995; 36:783.

[6] Hirano S, Yamamoto K, Inui H. *Energy Convers Mgmt* 1997; 38:5517.

[7] Kondo, J. Inui, T. and Wasa, K (Eds). Proceedings of the 2nd International Conference on Carbon Dioxide Removal, Pergamon Press, 1995.

[8] Riley JP and Skirow G. (1975) *Chemical Oceanography* Academic Press, New York, 1975.

[9] Hirano S, Yamamoto K, Inui H, Ji M, Zhang M. *Macromol Symp* 1996; 105:149-154.

[10] Hirano S, Yamamoto K, Yamada M, Inui H. Ji. M. *Advan Chitin Sci* 1996; 1:137.

[11] Zhang S and Gonsalves KE. *J Appl Polym Sci* 1995; 56:687.

[12] Bitter T and Muir H. *Anal Biochem* 1962; 4:330.

[13] Hirano S. *Applications of Chitin and Chitosan* (Ed MFA Goosen), Technomic, Lancaster 1997; 237-258.